Sparseness-controlled Adaptive Algorithms for Echo Cancellation

Pradeep Loganathan

December 2008

A report submitted in fulfilment of requirements for the MPhil to PhD transfer examination.

Communications and Signal Processing Group
Dept of Electrical and Electronic Engineering
Imperial College London

Abstract

In hands-free telephony, the acoustic coupling between the loudspeaker and the microphone generates echoes that can seriously degrade user experience. For this reason, effective Acoustic echo cancellation (AEC) is important to maintaining and improving the perceived voice quality of a call.

Traditionally, adaptive filters have been deployed in acoustic echo cancellers to estimate the Acoustic impulse response s (AIRs) using adaptive algorithms. The performances of a range of algorithms, including Normalized least-mean-square (NLMS), Proportionate normalized least-mean-square (PNLMS), μ-law proportionate normalized least-mean-square (MPNLMS) and Improved proportionate normalized least-mean-square (IPNLMS), are studied in the context of both AEC and Network echo cancellation (NEC). This analysis presents insights into their tracking performances under both time-invariant and time-varying system conditions.

In the context of AEC, it is shown that the level of sparseness in AIRs can vary greatly in a mobile environment. When the response is strongly sparse, convergence of conventional approaches is poor. Drawing on techniques originally developed for NEC, we propose a class of AEC algorithms that can not only work well in both sparse and dispersive circumstances, but also adapt dynamically to the level of sparseness using a new sparseness-controlled approach. Simulation results, using White Gaussian noise (WGN) and speech input signals, show improved performance over existing methods. The proposed algorithms achieve these improvements with only a modest increase in computational complexity.

Contents

List of Figures

List of Tables

Abbreviations

AEC:	Acoustic echo cancellation
AIR:	Acoustic impulse response
CPNLMS:	Composite proportionate NLMS and NLMS
DTD:	Double talk detector
ERLE:	Echo return loss enhancement
FIR:	Finite impulse response
IPNLMS:	Improved proportionate normalized least-mean-square
LMS:	Least-mean-square
LRMS:	Loudspeaker-room-microphone system
MPNLMS:	μ-law proportionate normalized least-mean-square
MSE:	Mean square error
NEC:	Network echo cancellation
NLMS:	Normalized least-mean-square
PNLMS:	Proportionate normalized least-mean-square
PNLMS++:	Proportionate normalized least-mean-square++
PSTN:	Public switched telephone network
SC-IPNLMS:	Sparseness-controlled improved proportionate NLMS
SC-MPNLMS:	Sparseness-controlled μ-law proportionate NLMS
SC-PNLMS:	Sparseness-controlled proportionate NLMS
SPNLMS:	Segment proportionate NLMS
SNR:	Signal-to-noise ratio
VoIP:	Voice over internet protocol
WGN:	White Gaussian noise

List of Symbols

$[.]^T$:	Matrix transpose operator
$\mathbf{I}_{m\times n}$:	Identity matrix of dimension m rows $\times n$ columns
$E\{.\}$:	Expectation operator
$\|.\|_2^2$:	Squared l_2-norm
n :	Sample iteration
L :	Length of adaptive filter
L_T :	Length of transmission room impulse response
L_R :	Length of receiving room impulse response
$s_T(n)$:	Transmission room source
$s_R(n)$:	Receiving room source
$y(n)$:	Receiving room signal
$\hat{y}(n)$:	Adaptive filter output
$e(n)$:	*a priori* error
$w(n)$:	Uncorrelated measurement noise
$\mathbf{Q}(n)$:	Diagonal tap selection control matrix
$\mathcal{J}(n)$:	Cost function
$\mathbf{h}(n)$:	True room impulse response
$\hat{\mathbf{h}}(n)$:	Estimated room impulse response
$\mathbf{x}(n)$:	Tap input vector
σ_x^2 :	Variance of input signal

σ_s^2 : Variance of the added noise in Markov model

β : Control parameter for Markov model

δ : Regularization parameter

μ : Step-size parameter

ξ : Control parameter for non-stationary unknown impulse response

List of Submissions

The following papers have been written during the course of my first year:

Published Paper

- Pradeep Loganathan, Andy W. H Khong and Patrick A. Naylor, "A Sparseness-controlled Proportionate Algorithm for Acoustic Echo Cancellation," *Proc. European Signal Processing Conference*, 2008.

Submitted paper

- A Journal, titled "A Class of Sparseness-controlled Algorithms for Echo Cancellation," was submitted to IEEE Transactions on Audio, Speech and Language Processing on 9 September 2008.

Chapter 1

Introduction

1.1 Overview

Wireless phones are increasingly being regarded as essential communications tools due to their flexibility. As the use for the in-car hands free telephony has gained much popularity in recent years due to the rise in safety concerns, and also the need for an automated service delivery system, digital wireless subscribers are becoming ever more critical of the voice quality they receive from network providers. One factor that affects the voice quality is echo.

An echo is said to occur when delayed and possibly distorted versions of a signal are reflected back to the source of that signal. Acoustic echo is a type of echo which is produced by poor voice coupling between the earpiece and microphone in handsets and hands-free devices. As shown in Fig. 1.1, sound signal, $\mathbf{x}(n)$, from a loudspeaker is heard by a listener, as intended. However, this same sound also is picked up by the microphone, both directly and indirectly, after bouncing off the wall. The result of this reflection is the creation of echo which is transmitted back to the far end and is heard by the talker as echo.

Hybrid echo is the other type of echo generated in the Public switched telephone network (PSTN) due to the impedance mismatch by the two-to-four wire conversion in the hybrid transformers. The network echo response in such systems is typically of length 64-128 ms, characterised by an unknown bulk delay dependant on network loading, encoding and jitter buffer delays [1]. This results in an 'active' region in the range of 8-12 ms

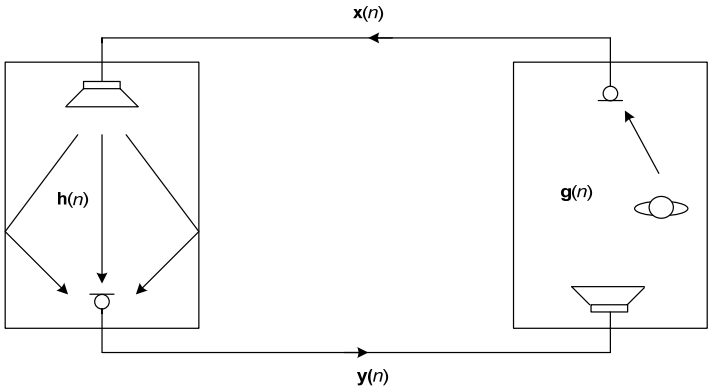

Figure 1.1: Illustration of acoustic echo in a Loudspeaker-Room-Microphone system (LRMS).

duration and consequently, the impulse response is dominated by 'inactive' regions where coefficient magnitudes are close to zero, making the impulse response sparse.

One of the earliest methods for echo cancellation in satellite communication is to insert echo suppression devices. They were voice-activated switches that transmitted a voice path and then turned off to block any echo signal. The main issue with these gadgets is that they eliminated double-talk capabilities (parties at both ends cant speak simultaneously).

Nowadays, adaptive filters are used in echo cancellers which model and subtracts the echo from the return path and therefore, outperformed the suppression-based technique. This technique is being crucial for many other applications in the field of telecommunication, such as noise cancellation and channel equalization [2]. Although adaptive filters can be used when the echo path is initially unknown, their application is unavoidable when facing varying environments.

Traditionally, echo cancellers are realized by a Finite impulse response (FIR) structure to achieve echo cancellation using algorithms such as the NLMS algorithm. For sparse systems such as encountered in NEC, the NLMS algorithm suffers from slow convergence and therefore new algorithms have been proposed for sparse adaptive filtering.

Several approaches have been proposed to overcome the NLMS weakness for NEC, including sparse adaptive algorithms, Fourier [3] and Wavelet [4] based adaptive algorithms, variable step-size (VSS) algorithm [5] [6] [7], data reusing technique [8] [9], partial update adaptive filtering techniques [10] [11] and sub-band adaptive filtering (SAF) schemes [12].

Sparse adaptive algorithms have been derived from NLMS to improve the performance in sparse system identification. These algorithms have also been proposed in frequency domains not only to exploit the computational efficiency of the fast Fourier transform to achieve fast convolution, but also to use the pseudo-orthogonality property of the discrete Fourier transform [13] to speed up the convergence rate. The VSS algorithm improves the performance of the adaptive algorithm by employing larger step-size at the beginning of the adaptation, for fast initial convergence, and a smaller step-size during later stage of adaptation, in order to achieve low mis-adjustment. The data reusing is another technique which was introduced to achieve improvement in convergence rate. This approach reuses the current desired response and data vector repeatedly to update the adaptive tap-weight vector several times during each iteration. Partial update algorithms are proposed to reduce the computational complexity of an adaptive filter by updating only a subset of filter coefficients for each iteration based on selection criteria. SAF has also been introduced in AEC to achieve complexity reduction whilst achieving an improved rate of convergence compared to the conventional full-band structure.

In this paper, we will devote our attention to sparse adaptive algorithms, as they are still of interest because of their ease of implementation, and the frame work that we will propose in this paper can be applied to most of the above techniques.

One of the first sparse adaptive filtering algorithms for NEC is PNLMS [14] in which each filter coefficient is updated with an independent step-size that is linearly proportional to the magnitude of that estimated filter coefficient. It is well known that PNLMS has very fast initial convergence for sparse impulse responses after which its convergence rate reduces significantly, sometimes resulting in a slower overall convergence than NLMS. In addition, PNLMS suffers from slow convergence when estimating dispersive impulse responses [15][16]. To address the latter problem, subsequent improved versions, such as PNLMS++ [15], were proposed. The PNLMS++ algorithm achieves improved convergence by alternating between NLMS and PNLMS for each sample period. However, as shown in [17], the PNLMS++ algorithm only performs best in the cases when the impulse response is sparse or highly dispersive.

An IPNLMS [17] algorithm was proposed to exploit the 'proportionate' idea by introducing a controlled mixture of proportionate (PNLMS) and non-proportionate (NLMS)

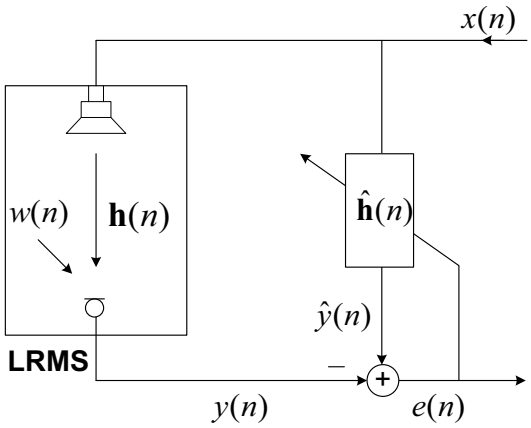

Figure 1.2: Adaptive system for acoustic echo cancellation in a Loudspeaker-Room-Microphone system (LRMS).

adaptation. A sparseness-controlled IPNLMS (SC-IPNLMS) algorithm was proposed in [18] to improve the robustness of IPNLMS to the sparseness variation in impulse responses. Composite proportionate NLMS and NLMS (CPNLMS) [19] adaptation was proposed to control the switching of PNLMS++ between the NLMS and PNLMS algorithms. For sparse impulse responses, CPNLMS performs the PNLMS adaptation to update the large coefficients and subsequently switches to NLMS, which has better performance for the adaptation of the remaining small taps. The MPNLMS [20] algorithm was proposed to address the uneven convergence rate of PNLMS during the estimation process. As proposed in [20], MPNLMS uses optimal step-size control factors to achieve faster overall convergence until the adaptive filter reaches its steady state.

The main limitation of all these adaptive algorithms is that their performances are subject to a tradeoff between the speed of convergence and high precision. Algorithms with higher step-size achieves faster convergence, but the mismatch between the true system and the predicted system is worse compared to that with smaller step-size. To overcome this tradeoff, a combination framework was proposed in [21], which adaptively combines two independent Least-mean-square (LMS) filters with large and small step sizes to obtain fast convergence with low mis-adjustment.

Although sparse adaptive filtering algorithms, such as those described above, have originally been developed for NEC, it has been shown in [22] that such algorithms give good convergence performance in the AEC system.

1.2 Problem formulation

The time variation of the near-end AIR, in the AEC system illustrated in Fig. 1.2, may arise due to, for example, a change in temperature [23], pressure and changes in the acoustic environment [24]. Variation in the sparseness of AIRs can also occur in AEC within an enclosed space.

We formulate the problem by considering an example case illustrated in Fig. 1.3, where the distance, a, between a loudspeaker and the user using, for example, a wireless microphone is varying. It shows two AIRs, generated using the method of images [25][26] using room dimensions of $8 \times 10 \times 3$ m and 0.57 as the reflection coefficient. The loudspeaker is fixed at $4 \times 9.1 \times 1.6$ m in the Loudspeaker-room-microphone system (LRMS) while the microphone is positioned at $4 \times 8.2 \times 1.6$ m and $4 \times 1.4 \times 1.6$ m giving impulse responses as shown in Fig. 1.3 (a) and (b) for $a = 0.9$ m and $a = 7.7$ m respectively. As can be seen, the sparseness of these AIRs varies with the loudspeaker-microphone distance. Hence, algorithms developed for mobile hands-free terminals are required to be robust to the variations in the sparseness of the acoustic path.

1.3 Report organization

The four chapters of this report are organized as follows:

Chapter 2 reviews the main adaptive algorithms for echo cancellation and presents a new class of algorithms that are robust to the sparseness variation of AIRs. These algorithms compute a sparseness measure of the estimated impulse response at each iteration of the adaptive process and incorporate it into their conventional methods. As will be shown, the proposed sparseness-controlled algorithms achieve fast convergence for both sparse and dispersive AIRs and are effective for AEC.

Chapter 3 details the planning and time-line for implementation of feasible future research areas.

Chapter 4 concludes remarks of this report.

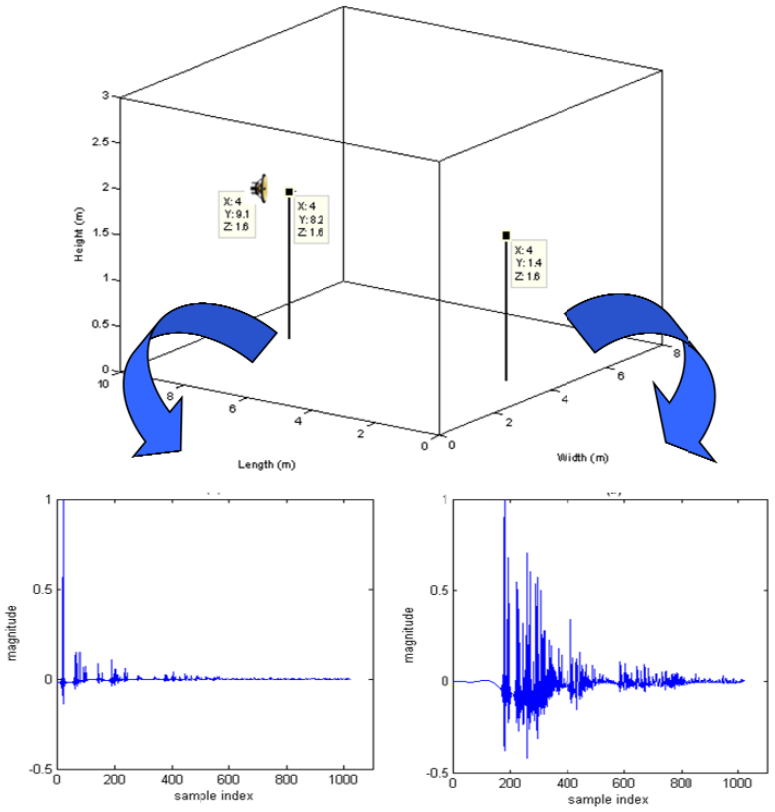

Figure 1.3: Loudspeaker-Room-Microphone system (LRMS) and two acoustic Impulse Responses, generated using the method of images, for the cases when the separation is 0.9 m and 7.7 m.

Chapter 2

Adaptive algorithms for echo cancellation

This chapter starts by reviewing the main conventional adaptive algorithms for echo cancellation, with introducing notations used throughout this report. A class of algorithms employing sparseness measure of the estimated impulse response is formulated in Section 2.2. The computational complexity of the proposed algorithms are discussed in Section 2.4, while simulation results comparing their performances under stationary and non-stationary environment are presented in Section 2.5 and Section 2.6.2, respectively.

2.1 Review of algorithms for echo cancellation

Figure 1.2 shows a LRMS and an adaptive filter $\widehat{\mathbf{h}}(n) = [\widehat{h}_0(n)\widehat{h}_1(n)\dots\widehat{h}_{L-1}(n)]^T$ deployed to cancel acoustic echo, where L is the length of the adaptive filter assumed to be equal to the unknown room impulse response and $[\cdot]^T$ is the transposition operator. Defining the input signal $\mathbf{x}(n) = [x(n)\ x(n-1)\ \dots\ x(n-L+1)]^T$ and $\mathbf{h}(n) = [h_0(n)\ h_1(n)\ \dots\ h_{L-1}(n)]^T$ as the unknown impulse response, the output of the LRMS is given by

$$y(n) = \mathbf{h}^T(n)\mathbf{x}(n) + w(n), \tag{2.1}$$

where $w(n)$ is additive noise and the error signal is given by

$$e(n) = y(n) - \widehat{\mathbf{h}}^T(n-1)\mathbf{x}(n). \tag{2.2}$$

Several adaptive algorithms such as those described below have been developed for either AEC or NEC.

Many adaptive algorithms can be described by (2.2) and the following set of equations:

$$\widehat{\mathbf{h}}(n) = \widehat{\mathbf{h}}(n-1) + \frac{\mu \mathbf{Q}(n-1)\mathbf{x}(n)e(n)}{\mathbf{x}^T(n)\mathbf{Q}(n-1)\mathbf{x}(n) + \delta}, \tag{2.3}$$

$$\mathbf{Q}(n-1) = \text{diag}\{q_0(n-1) \ \ldots \ q_{L-1}(n-1)\}, \tag{2.4}$$

where μ is a step-size and δ is the regularization parameter. The diagonal step-size control matrix $\mathbf{Q}(n)$ is introduced here to determine the step-size of each filter coefficient and is dependent on the specific algorithm.

2.1.1 The NLMS, PNLMS and MPNLMS algorithms

The NLMS algorithm is one of the most popular for AEC due to its straightforward implementation and low complexity compared to, for example, the recursive least squares algorithm. For NLMS, since the step-size is the same for all filter coefficients, $\mathbf{Q}(n) = \mathbf{I}_{L\times L}$ with $\mathbf{I}_{L\times L}$ being an $L \times L$ identity matrix.

One of the main drawbacks of the NLMS algorithm is that its convergence rate reduces significantly when the impulse response is sparse, such as often occurs in NEC. The poor performance has been addressed by several sparse adaptive algorithms such as those described below that have been developed specifically to identify sparse impulse responses in NEC applications.

The PNLMS [14] and MPNLMS [20] algorithms have been proposed for sparse system identification. Diagonal elements q_l of the step-size control matrix $\mathbf{Q}(n)$ for the PNLMS and MPNLMS algorithms can be expressed as

$$q_l(n) = \frac{\kappa_l(n)}{\frac{1}{L}\sum_{i=0}^{L-1}\kappa_i(n)}, \qquad 0 \le l \le L-1, \tag{2.5}$$

$$\begin{aligned} k_l(n) = \max\Big\{ & \rho \times \max\{\gamma, \\ & F(|\widehat{h}_0(n)|) \ \ldots \ F(|\widehat{h}_{L-1}(n)|)\}, F(|\widehat{h}_l(n)|)\Big\}, \end{aligned} \tag{2.6}$$

where $F(|\widehat{h}_l(n)|)$ is specific to the algorithm. The parameter $\gamma = 0.01$ in (2.6) prevents the filter coefficients $\widehat{h}_l(n)$ from stalling when $\widehat{\mathbf{h}}(0) = \mathbf{0}_{L\times 1}$ at initialisation and ρ, with a

typical value of 0.01, prevents the coefficients from stalling when they are much smaller than the largest coefficient.

The PNLMS algorithm achieves a high rate of convergence by employing step-sizes that are proportional to the magnitude of the estimated impulse response coefficients where elements $F(|\widehat{h}_l(n)|)$ are given by

$$F(|\widehat{h}_l(n)|) = |\widehat{h}_l(n)|. \tag{2.7}$$

Hence, PNLMS employs larger step-sizes for 'active' coefficients than for 'inactive' coefficients and consequently achieves faster convergence than NLMS for sparse impulse responses. However, it is found that PNLMS achieves fast initial convergence followed by a slower second phase convergence [20].

The MPNLMS algorithm was proposed to improve the convergence of PNLMS. It achieves this by computing the optimal proportionate step-size during the adaptation process. The MPNLMS algorithm was derived such that all coefficients attain a converged value to within a vicinity ϵ of their optimal value in the same number of iterations [20]. As a consequence, $F(|\widehat{h}_l(n)|)$ for MPNLMS is specified by

$$F(|\widehat{h}_l(n)|) = \ln(1 + \beta|\widehat{h}_l(n)|), \tag{2.8}$$

with $\beta = 1/\epsilon$ and ϵ is a very small positive number chosen as a function of the noise level [20]. It has been shown that $\epsilon = 0.001$ is a good choice for typical echo cancellation. The positive bias of 1 in (2.8) is introduced to avoid numerical instability during the initialization stage when $|\widehat{h}_l(0)| = 0$, $\forall l$.

It is important to note that both PNLMS and MPNLMS suffer from slow convergence when the unknown system $\mathbf{h}(n)$ is dispersive [15][16]. This is because when $\mathbf{h}(n)$ is dispersive, $k_l(n)$ in (2.6) becomes significantly large for most $0 \leq l \leq L-1$. As a consequence, the denominator of $q_l(n)$ in (2.5) is large, giving rise to a small step-size for each large coefficient. This causes a significant degradation in convergence performance for PNLMS and MPNLMS when the impulse response is dispersive such as can occur in AIRs.

2.1.2 The IPNLMS algorithm

The IPNLMS [17] algorithm was originally developed for NEC and was further developed for the identification of acoustic room impulse responses [22]. It employs a combination of proportionate (PNLMS) and non-proportionate (NLMS) adaptation, with the relative significance of each controlled by a factor α_{IP} such that the diagonal elements of $\mathbf{Q}(n)$ are given as

$$q_l(n) = \frac{1-\alpha_{\mathrm{IP}}}{2L} + \frac{(1+\alpha_{\mathrm{IP}})|\widehat{h}_l(n)|}{2\|\widehat{\mathbf{h}}(n)\|_1 + \delta_{\mathrm{IP}}}, \qquad 0 \leq l \leq L-1. \tag{2.9}$$

where $\|\cdot\|_1$ is defined as the l_1-norm and the first and second terms are the NLMS and the proportionate terms respectively. It can be seen that IPNLMS is the same as NLMS when $\alpha_{\mathrm{IP}} = -1$ and PNLMS when $\alpha_{\mathrm{IP}} = 1$. Use of a higher weighting for NLMS adaptation, such as $\alpha_{\mathrm{IP}} = 0$, -0.5 or -0.75, is a favorable choice for most AEC/NEC applications [17]. It has been shown that, although the IPNLMS algorithm has faster convergence than NLMS and PNLMS regardless of the impulse response nature [17], we note from our simulations that it does not outperform MPNLMS for highly sparse impulse responses with the above choices of α_{IP}.

2.2 Characterisation of framework for robust convergence

In this Section, we quantify the degree of sparseness in AIRs. We provide an illustrative example to show how the sparseness of AIRs varies with the loudspeaker-microphone distance in an enclosed space such as when the user is using a wireless microphone for tele/video conferencing. This serves as a motivation for us to develop new algorithms which are robust to the sparseness variation of AIRs in the next Section. In addition, we also demonstrate how the choice of ρ in (2.6) affects the step-size of each filter coefficient for PNLMS.

2.2.1 Variation of sparseness in AIRs

The degree of sparseness for an impulse response can be quantified by [18][27]

$$\xi(n) = \frac{L}{L-\sqrt{L}} \left\{ 1 - \frac{\|\mathbf{h}(n)\|_1}{\sqrt{L}\,\|\mathbf{h}(n)\|_2} \right\} \tag{2.10}$$

It can be shown [18][27] that $0 \leq \xi(n) \leq 1$. In the extreme but unlikely case when

$$h_l(n) = \begin{cases} \pm k, & l = l_1, \\ 0, & 0 \leq l \leq L-1,\ l \neq l_1, \end{cases} \tag{2.11}$$

where $l_1 \in \{[0, L-1]\}$ and $k \in \Re$, then $\xi(n) = 1$. On the other hand, when $h_l(n) = \pm k\ \forall l$, then $\xi(n) = 0$, as shown in Fig. 2.1. In reality $\mathbf{h}(n)$ and hence $\xi(n)$ is time-varying and depends on factors such as temperature, pressure and reflectivity [23]. As explained before, the sparseness of AIRs $\xi(n)$ varies with the location of the receiving device in an open or enclosed environment. We will show how $\xi(n)$ can also vary with the loudspeaker-microphone distance in an enclosed space.

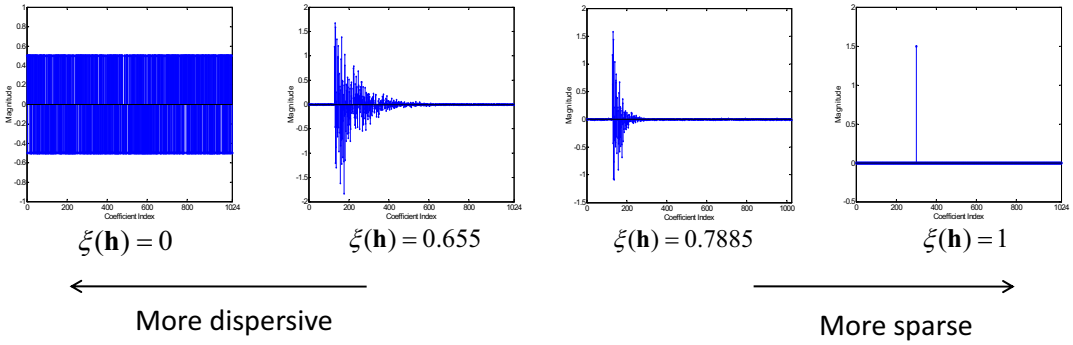

Figure 2.1: Sparseness measure of different impulse responses.

Consider an example case where the distance, a, between a fixed position loudspeaker and the talker using a wireless microphone is varying. Figure 2.2 illustrates how $\xi(n)$ of such AIRs varies with a for a room of dimension $8 \times 10 \times 3$ m and the loudspeaker is placed at $4 \times 9.1 \times 1.6$ m. In this illustrative example, the AIRs are generated using the method of images [25][26] with 1024 coefficients. For each loudspeaker-microphone distance a, the microphone is directly in front of the loudspeaker. As can be seen, $\xi(n)$ reduces with increasing a, since for increasing a, the sound field becomes more diffuse. Since $\xi(n)$ varies with a, we propose to incorporate $\xi(n)$ into PNLMS, MPNLMS and IPNLMS in order to improve their robustness to the sparseness of AIRs in AEC. Since $\mathbf{h}(n)$ is unknown during adaptation, we employ $\widehat{\xi}(n)$ to estimate the sparseness of an impulse response, where at each sample iteration,

$$\widehat{\xi}(n) = \frac{L}{L - \sqrt{L}} \left\{ 1 - \frac{\|\widehat{\mathbf{h}}(n)\|_1}{\sqrt{L}\ \|\widehat{\mathbf{h}}(n)\|_2} \right\}. \tag{2.12}$$

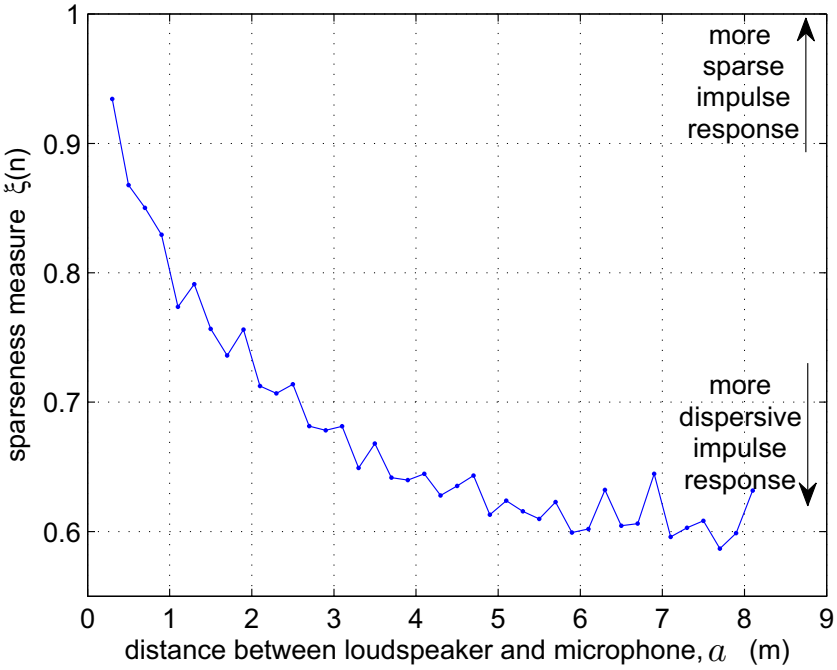

Figure 2.2: Sparseness measure against the distance between loudspeaker and microphone, a. The impulse responses are obtained from the image model using a fixed room dimensions of $8 \times 10 \times 3$ m.

2.2.2 Effect of ρ on step-size control matrix $\mathbf{Q}(n)$ for PNLMS

As explained in Section 2.1.1, the parameter ρ in (2.6) was originally introduced to prevent freezing of the filter coefficients when they are much smaller than the largest coefficient. Figure 2.3 shows the effect of ρ for both sparse and dispersive AIRs on the convergence performance of PNLMS measured using the normalized misalignment defined by

$$\eta(n) \;=\; \frac{\|\mathbf{h}(n) - \widehat{\mathbf{h}}(n)\|_2^2}{\|\mathbf{h}(n)\|_2^2}. \tag{2.13}$$

A zero mean WGN sequence is used as the input signal while another WGN sequence $w(n)$ is added to give an Signal-to-noise ratio (SNR) of 20 dB. Impulse responses as shown in Fig. 1.3 (a) and (b) are used as sparse and dispersive AIRs, and $\mu_{\text{PNLMS}} = 0.3$. It can be seen from this illustration that, for a sparse $\mathbf{h}(n)$, we desire a low value of ρ while, for a dispersive unknown system $\mathbf{h}(n)$, we desire a high value of ρ. This is due to the resulting effect of how different values of ρ affect the step-size control element $q_l(n)$ as illustrated in Fig. 2.4. It can be observed that a higher value of ρ will reduce the influence of the proportional update term meaning that all filter coefficients are updated

at a more uniform rate. This provides a good convergence performance for PNLMS for a dispersive AIR. On the other hand, a lower ρ will increase the degree of proportionality hence giving good convergence performance when the AIR is sparse. As a consequence of this important observation, we propose to incorporate $\widehat{\xi}(n)$ into ρ for both PNLMS and MPNLMS as described in the next section.

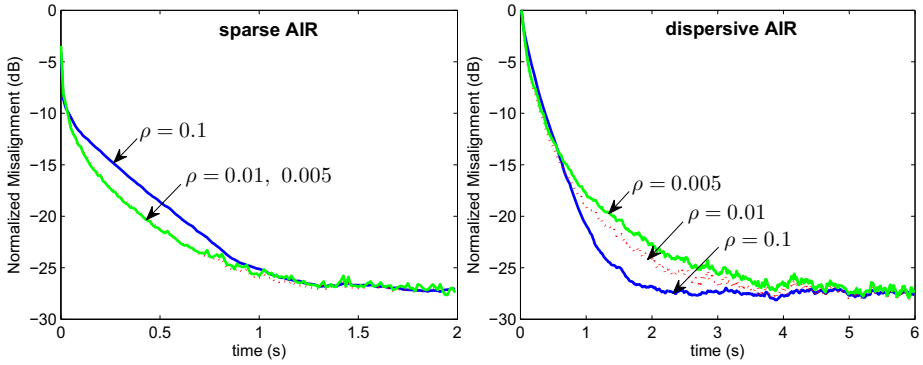

Figure 2.3: Convergence of the PNLMS for different values of ρ using WGN input signal. Impulse responses in Fig. 1.3 (a) and (b) are used as sparse and dispersive AIRs respectively. [$\mu_{\text{PNLMS}} = 0.3$, SNR = 20 dB]

2.3 A class of Sparseness-controlled algorithms

We propose to improve the robustness of PNLMS, MPNLMS and IPNLMS to varying levels of sparseness of impulse response such as encountered in, for example, AEC. As will be shown in the following, this is achieved by incorporating the sparseness measure of the estimated AIRs into the adaptation process.

2.3.1 The proposed SC-PNLMS and SC-MPNLMS algorithms

In order to address the problem of slow convergence in PNLMS and MPNLMS for dispersive AIR, we require the step-size control elements $q_l(n)$ to be robust to the sparseness of the impulse response. Several choices can be employed to obtain the desired effect of achieving a high ρ when $\widehat{\xi}(n)$ is small when estimating dispersive AIRs. We consider an example function

$$\rho(n) = e^{-\lambda\widehat{\xi}(n)}, \qquad \lambda \in \mathbb{R}^{+}. \tag{2.14}$$

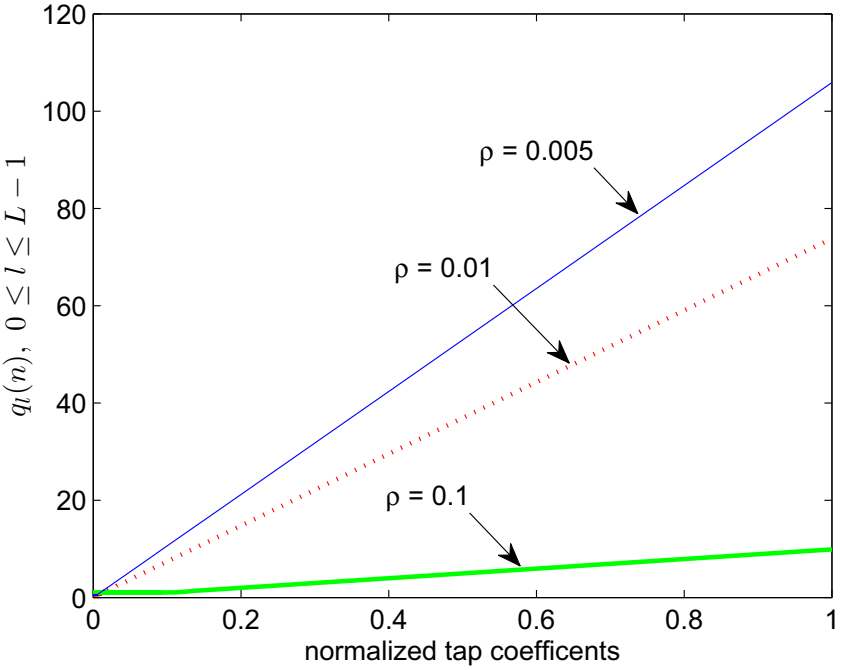

Figure 2.4: Magnitude of $q_l(n)$ for $0 \leq l \leq L-1$ against the magnitude of coefficients $\widehat{h}_l(n)$ in PNLMS.

The variation of $\rho(n)$ in PNLMS for the exponential function is plotted in Fig. 2.5 for the cases where $\lambda = 4, 6$ and 8. It can be noted that a linear function $\rho(n) = 1 - \widehat{\xi}(n)$ also achieves our desired condition. We have tested this case and found it to perform worse than the more general form of (2.14), so we will not consider it further.

It can be seen that low values of $\rho(n)$ are allocated for a large range of sparse impulse responses such as when $\widehat{\xi}(n) > 0.4$. As a result of small values in $\rho(n)$ using (2.14), the proposed sparseness-controlled PNLMS algorithm (SC-PNLMS) inherits the proportionality step-size control over a large range of sparse impulse response. When the impulse response is dispersive, such as when $\widehat{\xi}(n) < 0.4$, the proposed SC-PNLMS algorithm inherits the NLMS adaptation control with larger values of $\rho(n)$. As explained in Section 2.2.2 and Fig. 2.4, this gives a more uniform step-size across $h_l(n)$. Hence, the exponential function described by (2.14) will achieve our overall desired effect of the robustness to sparse and dispersive AIRs.

The choice of λ is important. As can be seen from Fig. 2.5, a larger choice of λ will cause the proposed SC-PNLMS to inherit more of PNLMS properties compared to NLMS giving good convergence performance when AIR is sparse. On the other hand, when the

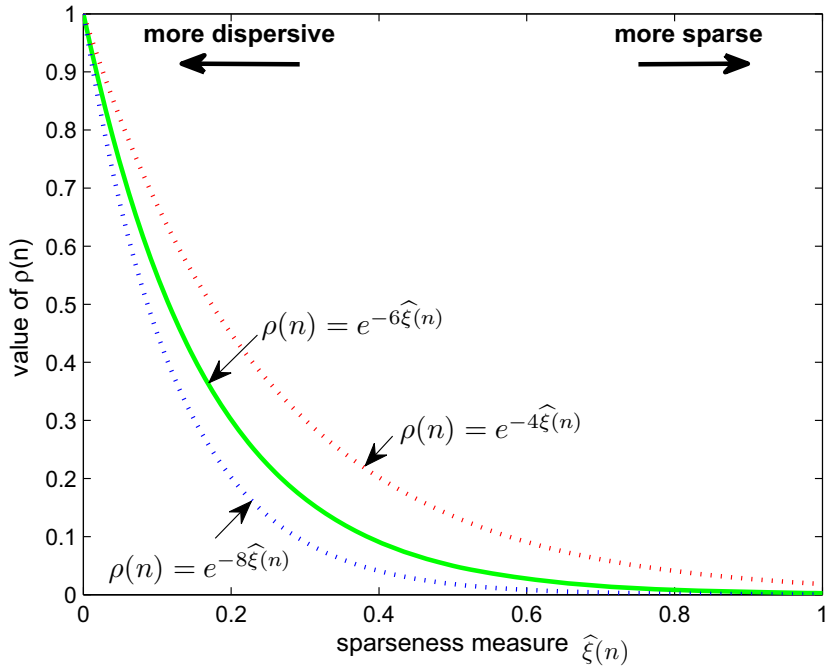

Figure 2.5: Variation of ρ against sparseness measure $\widehat{\xi}(n)$ of impulse response.

AIR is dispersive, λ must be small for good convergence performance. Hence, we show in Section 2.5.1 that a good compromise is given by $\lambda = 6$, though the algorithm is not very sensitive to this choice in the range of $4 \leq \lambda \leq 6$.

Incorporating $\rho(n)$ in a similar manner for the MPNLMS algorithm, the resulting sparseness-controlled MPNLMS algorithm (SC-MPNLMS) inherits more of the MPNLMS properties when the estimated AIR is sparse and distributes uniform step-size across $h_l(n)$, as in NLMS, when the estimated AIR is dispersive. In addition, we note that when $n = 0$, $\|\widehat{\mathbf{h}}(0)\|_2 = 0$ and hence, to prevent division by a small number or zero, $\widehat{\xi}(n)$ can be computed for $n \geq L$ in both SC-PNLMS and SC-MPNLMS. When $n < L$, we set $\rho(n) = 5/L$ as described in [17]. The SC-PNLMS algorithm is thus described by (2.2)-(2.7), (2.12) and (2.14), whereas SC-MPNLMS is described by (2.2)-(2.6), (2.8), (2.12) and (2.14) with $\lambda = 6$, as summarised in Table 2.1.

2.3.2 The SC-IPNLMS algorithm

We choose to incorporate sparseness-control into the IPNLMS algorithm (SC-IPNLMS) [18] in a different manner compared to SC-PNLMS and SC-MPNLMS because,

Table 2.1: The Sparseness-controlled Algorithms

Initialisations:

$$\widehat{\mathbf{h}}(0) = \mathbf{0}_{L\times 1}$$
$$0 < \mu \leq 1$$
$$\alpha_{\mathrm{SC-IP}} = -0.75 \qquad \text{(SC-IPNLMS)}$$
$$\lambda = 6 \qquad \text{(SC-PNLMS, SC-MPNLMS)}$$
$$\rho(n) = 5/L, \quad n < L \qquad \text{(SC-PNLMS, SC-MPNLMS)}$$
$$\beta = 1000 \qquad \text{(SC-MPNLMS)}$$

General Computations:

$$e(n) = y(n) - \widehat{\mathbf{h}}^T(n-1)\mathbf{x}(n)$$
$$\widehat{\mathbf{h}}(n) = \widehat{\mathbf{h}}(n-1) + \frac{\mu\mathbf{Q}(n-1)\mathbf{x}(n)e(n)}{\mathbf{x}^T(n)\mathbf{Q}(n-1)\mathbf{x}(n) + \delta}$$
$$\mathbf{Q}(n-1) = \mathrm{diag}\{q_0(n-1), \ldots, q_{L-1}(n-1)\}$$
$$\widehat{\xi}(n) = \frac{L}{L-\sqrt{L}}\left\{1 - \frac{\|\widehat{\mathbf{h}}(n)\|_1}{\sqrt{L}\,\|\widehat{\mathbf{h}}(n)\|_2}\right\}, \qquad n \geq L$$

SC-PNLMS

$$q_l(n) = \frac{\kappa_l(n)}{\frac{1}{L}\sum_{i=0}^{L-1}\kappa_i(n)}, \qquad 0 \leq l \leq L-1$$
$$k_l(n) = \max\Big\{\rho(n) \times \max\{\gamma, |\widehat{h}_0(n)|, \ldots, |\widehat{h}_{L-1}(n)|\}, |\widehat{h}_l(n)|\Big\}$$
$$\rho(n) = e^{-\lambda\widehat{\xi}(n)}, \qquad n \geq L$$

SC-MPNLMS

$$q_l(n) = \frac{\kappa_l(n)}{\frac{1}{L}\sum_{i=0}^{L-1}\kappa_i(n)}, \qquad 0 \leq l \leq L-1$$
$$k_l(n) = \max\Big\{\rho(n) \times \max\{\gamma, \mathrm{F}(|\widehat{h}_0(n)|), \ldots, \mathrm{F}(|\widehat{h}_{L-1}(n)|)\}, \mathrm{F}(|\widehat{h}_l(n)|)\Big\}$$
$$\mathrm{F}(|\widehat{h}_l(n)|) = \ln(1 + \beta|\widehat{h}_l(n)|)$$
$$\rho(n) = e^{-\lambda\widehat{\xi}(n)}, \qquad n \geq L$$

SC-IPNLMS

$$q_l(n) = \Big[\frac{1 - 0.5\widehat{\xi}(n)}{L}\Big]\frac{(1-\alpha_{\mathrm{SC-IP}})}{2L} + \Big[\frac{1 + 0.5\widehat{\xi}(n)}{L}\Big]\frac{(1+\alpha_{\mathrm{SC-IP}})|\widehat{h}_l(n)|}{2\|\widehat{\mathbf{h}}(n)\|_1 + \delta_{\mathrm{IP}}}$$

as can be seen from (2.9), two terms are employed in IPNLMS for control of the mixture between proportionate and NLMS updates. The proposed SC-IPNLMS improves the performance of the IPNLMS by expressing $q_l(n)$ for $n \geq L$ as

$$q_l(n) = \left[\frac{1 - 0.5\widehat{\xi}(n)}{L}\right] \frac{(1 - \alpha_{\text{SC-IP}})}{2L} + \left[\frac{1 + 0.5\widehat{\xi}(n)}{L}\right] \frac{(1 + \alpha_{\text{SC-IP}})|\widehat{h}_l(n)|}{2\|\widehat{\mathbf{h}}(n)\|_1 + \delta_{\text{IP}}}. \tag{2.15}$$

As can be seen, for large $\widehat{\xi}(n)$ when the impulse response is sparse, the algorithm allocates more weight to the proportionate term of (2.9). For comparatively less sparse impulse responses, the algorithm aims to achieve the convergence of NLMS by applying a higher weighting to the NLMS term. An empirically chosen weighting of 0.5 in (2.15) is included to balance the performance between sparse and dispersive cases. In addition, normalization by L is introduced to reduce significant coefficient noise when the effective step-size is large for sparse AIRs with high $\widehat{\xi}(n)$.

Figure 2.6 illustrates the step-size control elements $q_l(n)$ for SC-IPNLMS in estimating different unknown AIRs. As can be seen, for dispersive AIRs, SC-IPNLMS allocates a uniform step-size across $h_l(n)$ while, for sparse AIRs, the algorithm distributes $q_l(n)$ proportionally to the magnitude of the coefficients. As a result of this distribution, the SC-IPNLMS algorithm varies the degree of NLMS and proportionate adaptations according to the nature of the AIRs. In contrast, in standard IPNLMS the mixing coefficient α_{IP} in (2.9) is fixed *a priori*. The SC-IPNLMS algorithm is described by (2.2)-(2.4), (2.12) and (2.15), as specified in Table 2.1.

2.4 Computational Complexity

The relative complexity of NLMS, PNLMS, SC-PNLMS, IPNLMS, SC-IPNLMS, MPNLMS and SC-MPNLMS in terms of the total number of additions (A), multiplications (M), logarithm (Log) and comparisons (C) per iteration is assessed in Table 2.2. The additional complexity of the proposed sparseness-controlled algorithms, on top of their conventional method, arises from the computation of the sparseness measure $\widehat{\xi}(n)$. Given

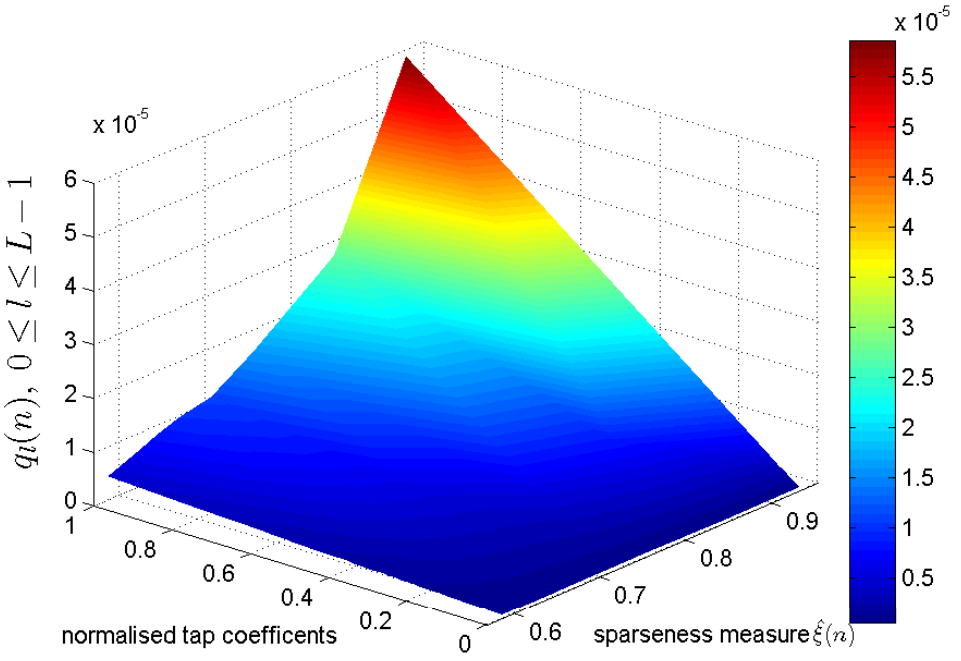

Figure 2.6: Magnitude of $q_l(n)$ for $0 \leq l \leq L-1$ against the magnitude of coefficients $\widehat{h}_l(n)$ in SC-IPNLMS and different sparseness measures of 8 systems.

that $L/(L-\sqrt{L})$ in (2.10) can be computed off-line, the remaining l-norms require an additional $2L$ additions and L multiplications. The SC-PNLMS and SC-MPNLMS algorithms additionally require computations for (2.14). Alternatively, a look-up table with values of $\rho(n)$ defined in (2.14) can be computed for $0 \leq \widehat{\xi}(n) \leq 1$. Segment PNLMS (SPNLMS) is proposed in [28], to approximate the μ-law function in MPNLMS using line segments. Since $\|\widehat{\mathbf{h}}(n)\|_1$ computation is already available from IPNLMS in (2.9), SC-IPNLMS only requires an additional $L+3$ additions and $L+7$ multiplications. The total computational complexity for an illustrative example of $L = 1024$ is given in Table 2.3.

2.5 Simulation Results

We present simulation results to evaluate the performance of the proposed SC-PNLMS, SC-MPNLMS and SC-IPNLMS algorithms in the context of AEC. In addition, we show an example case of how SC-IPNLMS can be employed in NEC. Throughout our simulations, algorithms were tested using a zero mean WGN and a male speech signal as inputs while another WGN sequence $w(n)$ is added to give an SNR of 20 dB. We assumed that the length of the adaptive filter $L = 1024$ is equivalent to that of the unknown system. Two

Table 2.2: Complexity of algorithms - Addition (A), Multiplication (M), Logarithm (Log) and Comparison (C).

Algorithm	A	M	Log	C
NLMS	$L+4$	$3L+2$	0	0
PNLMS	$2L+2$	$7L+3$	0	$2L$
SC-PNLMS	$4L+3$	$8L+6$	0	$2L$
IPNLMS	$3L+3$	$8L+2$	0	0
SC-IPNLMS	$4L+6$	$9L+9$	0	0
MPNLMS	$3L+2$	$8L+3$	L	$2L$
SC-MPNLMS	$5L+3$	$9L+6$	L	$2L$

Table 2.3: Complexity for the case of $L = 1024$ - Addition (A), Multiplication (M), Logarithm (Log) and Comparison (C).

Algorithm	A	M	Log	C
NLMS	1028	3074	0	0
PNLMS	2050	7171	0	2048
SC-PNLMS	4099	8198	0	2048
IPNLMS	3075	8194	0	0
SC-IPNLMS	4102	9225	0	0
MPNLMS	3074	8195	1024	2048
SC-MPNLMS	5123	9222	1024	2048

receiving room impulse responses $\mathbf{h}(n)$ for AEC simulations have been used as described in Fig. 1.3. The sparseness measure of these AIRs are computed using (2.10) giving (a) $\xi(n) = 0.83$ and (b) $\xi(n) = 0.59$ respectively.

2.5.1 Effect of λ on the performance of SC-PNLMS for AEC

SC-PNLMS was tested as shown in Fig. 2.7 for different λ values in (2.14) to illustrate the time taken to reach -20 dB normalized misalignment using a WGN sequence as the input signal. A step-size of $\mu = 0.3$ was used in this experiment. We see from the result that, for each case of λ, the SC-PNLMS has a higher rate of convergence for a sparse system compared to a dispersive system. This is due to the initialisation choice of $\widehat{\mathbf{h}}(0) = \mathbf{0}_{L\times 1}$, where most filter coefficients are initialized close to their optimal values. In addition, a smaller value of λ is favorable for the dispersive AIR, since SC-PNLMS performs similarly to NLMS for small λ values. On the contrary, a higher value for λ is desirable for the sparse case. It can be noted that SC-PNLMS is exactly NLMS for $\lambda = 0$. It can also be seen that a range of good value for λ is $4 \leq \lambda \leq 6$. Figure 2.8 shows the performance of SC-PNLMS with an echo path change introduced from Fig. 1.3 (a) to (b) at 4.5 s, for $\lambda = 0, 4, 6$ and 8. We observe from this result that the convergence rate of SC-PNLMS is high when λ is small for a dispersive channel. This is because, as explained in Section 2.3.1, the proposed algorithm inherits properties of the NLMS for a small λ value. For a high λ, the SC-PNLMS algorithm inherits properties of PNLMS giving good performance for sparse AIR before the echo path change. As can be seen, a good compromise of λ is given by $\lambda = 6$.

2.5.2 Convergence performance of SC-PNLMS for AEC

Figure 2.9 compares the performance of NLMS, PNLMS and SC-PNLMS using WGN as the input signal. The step-size parameter for each algorithm is chosen such that all algorithms achieve the same steady-state. This is achieved by setting $\mu_{\text{NLMS}} = \mu_{\text{PNLMS}} = \mu_{\text{SC-PNLMS}} = 0.3$. An echo path change was introduced from Fig. 1.3(a) to 1.3(b) while λ for the SC-PNLMS algorithm is set to 6. It can be seen from Fig. 2.9 that the convergence rate of SC-PNLMS is as fast as PNLMS for sparse and much better than PNLMS for dispersive, therefore achieving our objective of improving robustness to varying sparseness.

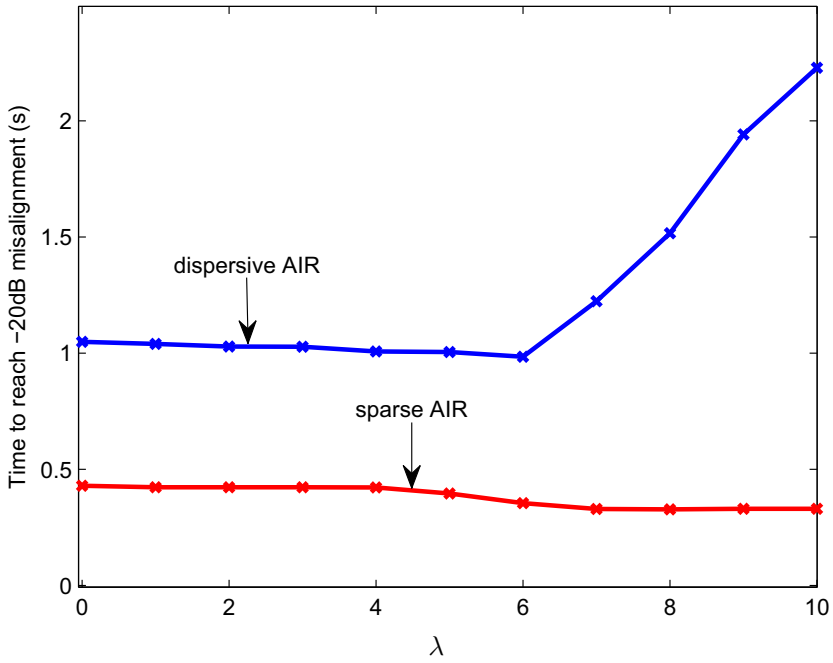

Figure 2.7: Time to reach -20 dB normalized misalignment level for different values of λ in SC-PNLMS using WGN input signal. Impulse response in Fig. 1.3 (a) and (b) used as sparse AIR and dispersive AIR respectively. [$\mu_{\text{SC-PNLMS}} = 0.3$, SNR = 20 dB]

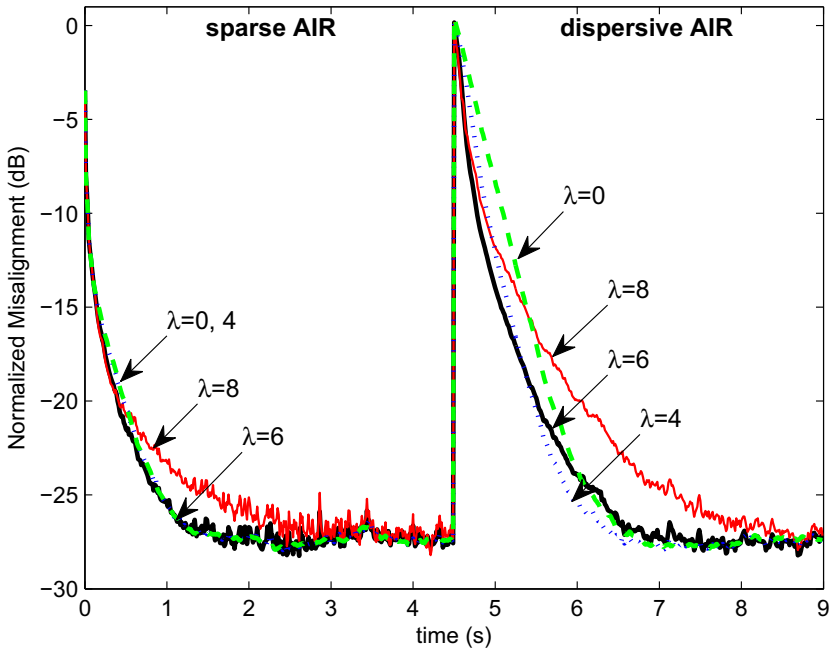

Figure 2.8: Convergence of the SC-PNLMS for different values of λ using WGN input signal with an echo path change at 4.5 s. Impulse response is changed from Fig. 1.3 (a) to (b) and $\mu_{\text{SC-PNLMS}} = 0.3$, SNR = 20 dB.

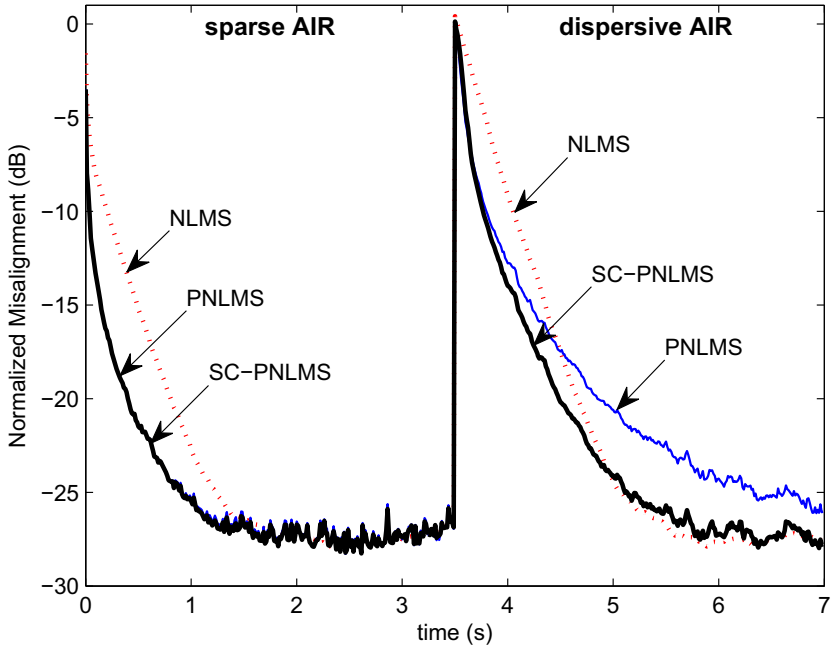

Figure 2.9: Relative convergence of NLMS, PNLMS and SC-PNLMS using WGN input signal with an echo path change at 3.5 s. Impulse response is changed from that shown from Fig. 1.3 (a) to (b) and $\mu_{\text{NLMS}} = \mu_{\text{PNLMS}} = \mu_{\text{SC-PNLMS}} = 0.3$, SNR = 20 dB.

This is because SC-PNLMS inherits the beneficial properties of both PNLMS and NLMS. It can be seen from the result that SC-PNLMS achieves high rate of convergence similar to PNLMS giving approximately 5 dB improvement in normalized misalignment during initial convergence compared to NLMS for a sparse AIR. After the echo path change, for a dispersive AIR, the SC-PNLMS maintains its high convergence rate over NLMS and PNLMS giving approximately 4 dB improvement in normalized misalignment compared to PNLMS.

Figure 2.10 shows simulation results for a male speech input signal where we used the same parameters as in the case of WGN input signal. As can be seen, the proposed SC-PNLMS algorithm achieves the highest rate of convergence, giving convergence as fast as PNLMS and approximately 7 dB improvement during initial convergence compared to NLMS for the sparse AIR. For dispersive AIR, SC-PNLMS performs almost the same as NLMS with approximately 4 dB improvement compared to PNLMS.

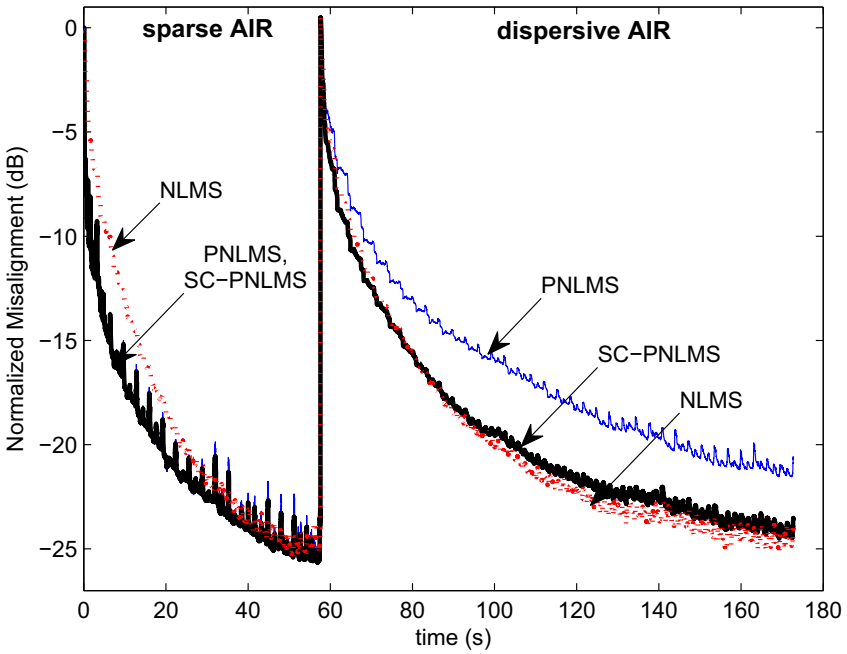

Figure 2.10: Relative convergence of NLMS, PNLMS and SC-PNLMS using speech input signal with echo path changes at 58 s. Impulse response is changed from that shown in Fig. 1.3 (a) to (b) and $\mu_{\text{NLMS}} = 0.3$, $\mu_{\text{PNLMS}} = \mu_{\text{SC-PNLMS}} = 0.1$, SNR = 20 dB.

2.5.3 Convergence performance of SC-MPNLMS for AEC

Figure 2.11 illustrates the performance of NLMS, MPNLMS and SC-MPNLMS using WGN as the input signal. As before, the step-sizes were adjusted to achieve the same steady-state misalignment for all algorithms. This corresponds to $\mu_{\text{NLMS}} = 0.3$, $\mu_{\text{MPNLMS}} = \mu_{\text{SC-MPNLMS}} = 0.25$. We have also used $\lambda = 6$ for SC-MPNLMS. As can be seen from this result, the SC-MPNLMS algorithm attains approximately 8 dB improvement in normalized misalignment during initial convergence compared to NLMS and same initial performance followed by approximately 2 dB improvement over MPNLMS for the sparse AIR. After the echo path change, SC-MPNLMS achieves approximately 3 dB improvement compared to MPNLMS and about 8 dB better performance than NLMS for dispersive AIR. As shown in Fig. 2.12, with speech signal as the input, the proposed SC-MPNLMS algorithm achieves approximately 10 dB improvement during initial convergence compared to NLMS and 2 dB compared to MPNLMS for the sparse AIR. For dispersive AIR, the SC-MPNLMS algorithm achieves an improvement of approximately 4 dB compared to both NLMS and MPNLMS.

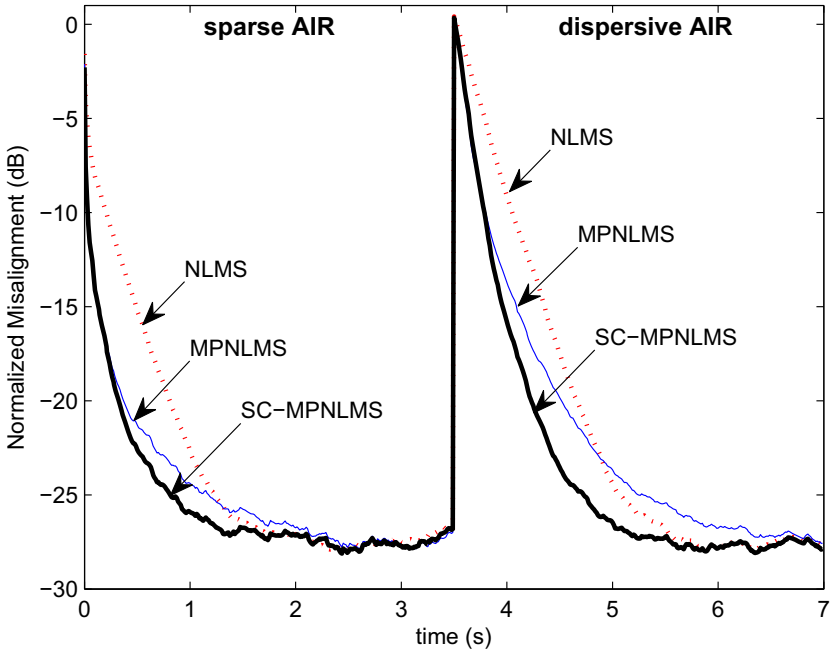

Figure 2.11: Relative convergence of NLMS, MPNLMS and SC-MPNLMS using WGN input signal with an echo path change at 3.5 s. Impulse response is changed from that shown from Fig. 1.3 (a) to (b) and $\mu_{\text{NLMS}} = 0.3$, $\mu_{\text{MPNLMS}} = \mu_{\text{SC-MPNLMS}} = 0.25$, SNR = 20 dB.

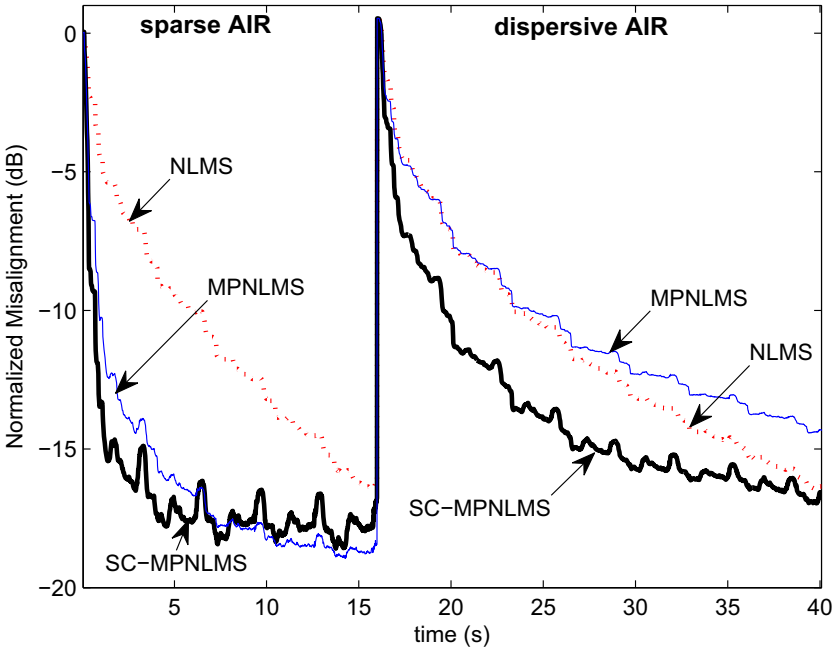

Figure 2.12: Relative convergence of NLMS, MPNLMS and SC-MPNLMS using speech input signal with echo path changes at 16 s. Impulse response is changed from that shown in Fig. 1.3 (a) to (b) and $\mu_{\text{NLMS}} = 0.3$, $\mu_{\text{MPNLMS}} = \mu_{\text{SC-MPNLMS}} = 0.25$, SNR = 20 dB.

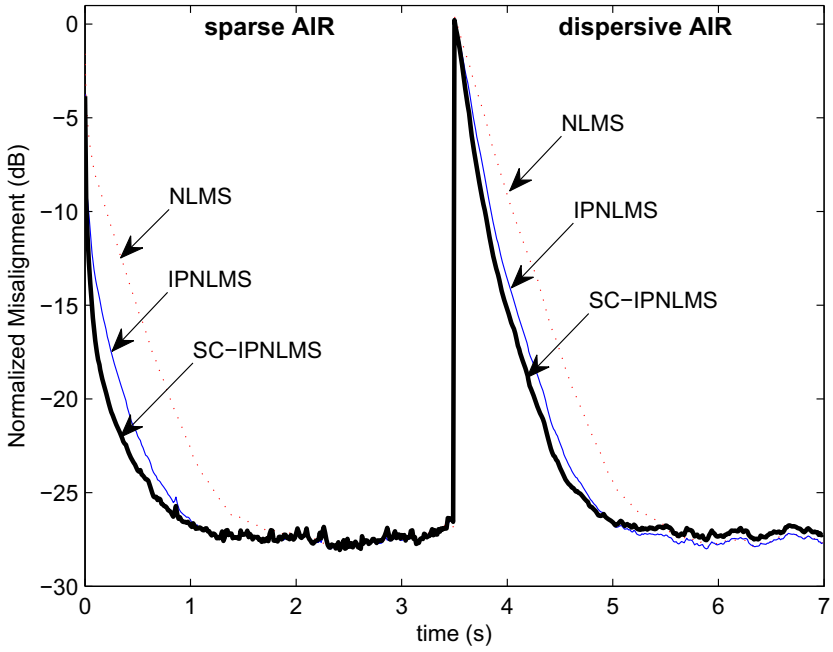

Figure 2.13: Relative convergence of NLMS, IPNLMS and SC-IPNLMS using WGN input signal with an echo path change at 3.5 s. Impulse response is changed from that shown from Fig. 1.3 (a) to (b) and $\mu_{\text{NLMS}} = \mu_{\text{IPNLMS}} = 0.3$, $\mu_{\text{SC-IPNLMS}} = 0.7$, SNR = 20 dB.

2.5.4 Convergence performance of SC-IPNLMS for AEC

For SC-IPNLMS performance comparison, we used $\mu_{\text{NLMS}} = \mu_{\text{IPNLMS}} = 0.3$, $\mu_{\text{SC-IPNLMS}} = 0.7$ in order to attain same steady state performance. Proportionality control factors $\alpha_{\text{IP}} = \alpha_{\text{SC-IP}} = -0.75$ have been used for both IPNLMS and SC-IPNLMS. It can be seen from Fig. 2.13 and 2.14 that by using both WGN and speech input signals, SC-IPNLMS achieves approximately 10 dB improvement in normalized misalignment during initial convergence compared to NLMS for the sparse AIR. For a dispersive AIR, the SC-IPNLMS achieves a 5 dB improvement compared to NLMS. For a speech input, the improvement of SC-IPNLMS over IPNLMS is 3 dB for both sparse and dispersive AIRs. On the other hand, the improvement of SC-IPNLMS compared to NLMS are 10 dB and 6 dB for sparse and dispersive AIRs, respectively.

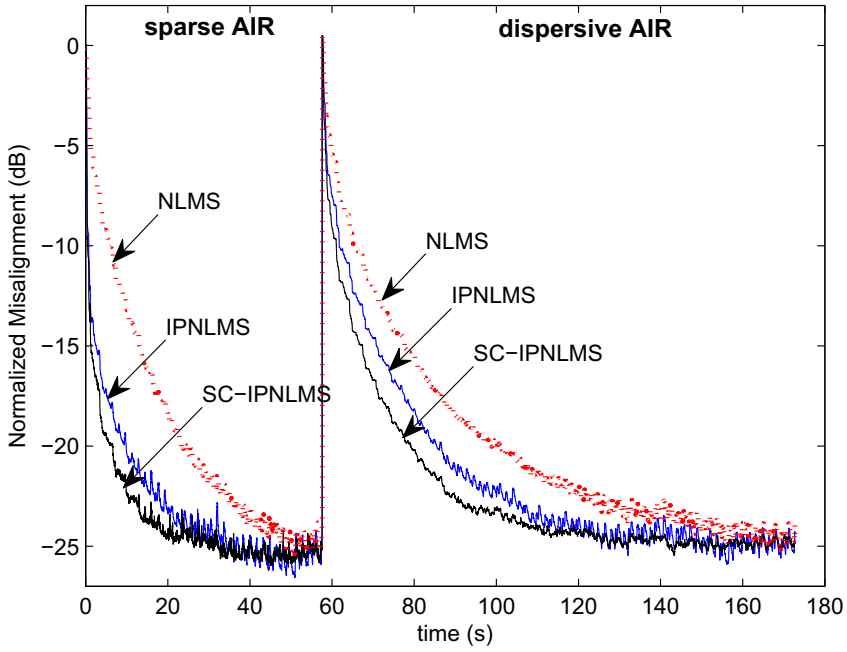

Figure 2.14: Relative convergence of NLMS, IPNLMS and SC-IPNLMS using speech input signal with echo path changes at 58 s. Impulse response is changed from that shown in Fig. 1.3 (a) to (b) and $\mu_{\text{NLMS}} = \mu_{\text{IPNLMS}} = 0.3$, $\mu_{\text{SC-IPNLMS}} = 0.8$, SNR = 20 dB.

2.5.5 Convergence performance of the algorithms for various AIRs with different sparseness in AEC

We extracted eight different impulse responses from the set of AIRs with sparseness measure $0.58 \leq \xi \leq 0.93$ as shown in Fig. 2.2. The time taken to reach -20 dB normalized misalignment is plotted against $\xi(n)$ for NLMS, PNLMS, SC-PNLMS, IPNLMS and SC-IPNLMS in Fig. 2.15, and for NLMS, MPNLMS and SC-MPNLMS in Fig. 2.16. As before, all step-sizes have been adjusted so that the algorithms achieve the same steady-state normalized misalignment. These correspond to $\mu_{\text{NLMS}} = \mu_{\text{PNLMS}} = \mu_{\text{SC-PNLMS}} = \mu_{\text{IPNLMS}} = 0.3$, $\mu_{\text{MPNLMS}} = \mu_{\text{SC-MPNLMS}} = 0.25$ and $\mu_{\text{SC-IPNLMS}} = 0.7$. It can be seen that when the AIRs are sparse, the speed of initial convergence increases significantly for each algorithm. This is because many of the filter coefficients are initialized close to their optimum values since during initialisation, $\widehat{\mathbf{h}}(0) = \mathbf{0}_{L\times 1}$. In addition, the sparseness-controlled algorithms (SC-PNLMS, SC-MPNLMS and SC-IPNLMS) give the overall best performance compare to their conventional methods across the range of sparseness measure. This is because the proposed algorithms take into account the sparseness measure of the estimated impulse response at each iteration.

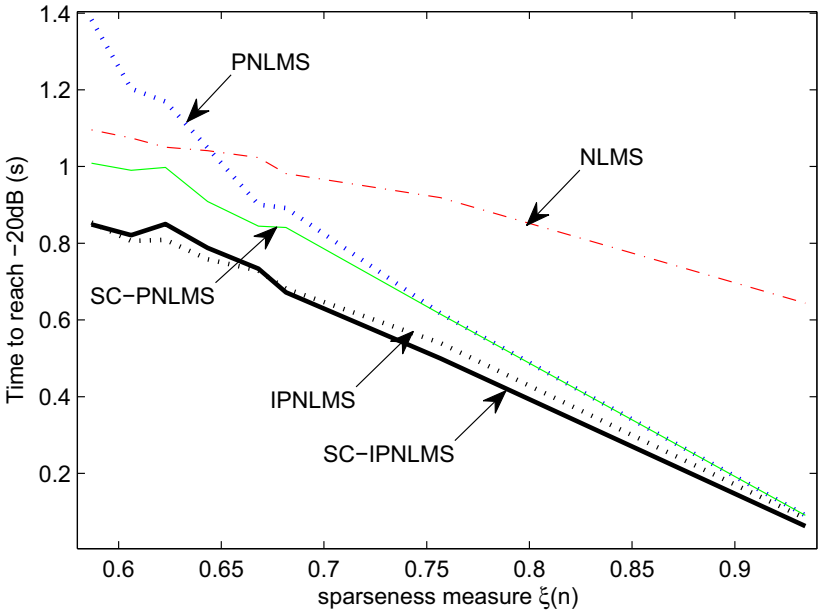

Figure 2.15: Time to reach the -20dB normalized misalignment against different sparseness measures of 8 systems for NLMS, PNLMS, SC-PNLMS, IPNLMS and SC-IPNLMS.

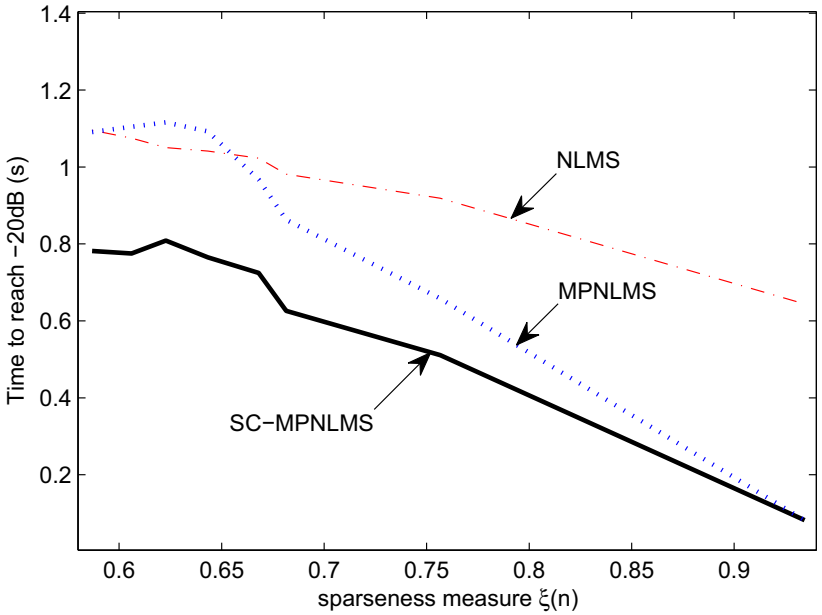

Figure 2.16: Time to reach the -20dB normalized misalignment against different sparseness measures of 8 systems for NLMS, MPNLMS and SC-MPNLMS.

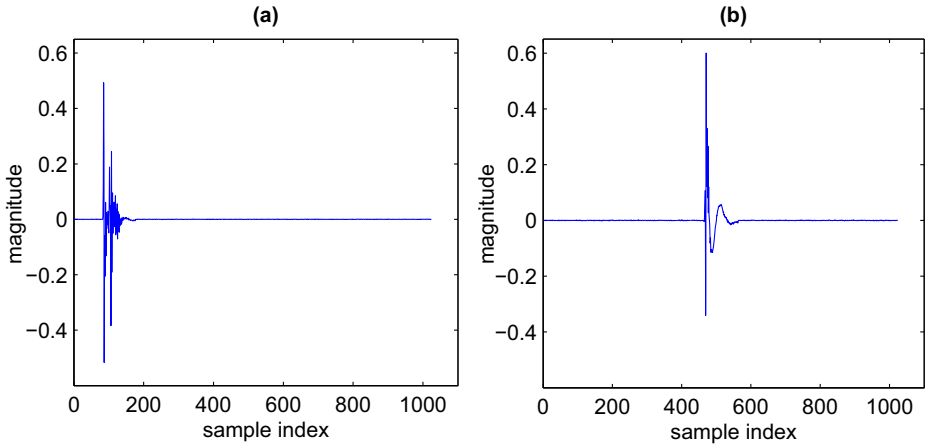

Figure 2.17: Sparse network impulse responses, sampled at 8 kHz, giving (a) $\xi(n) = 0.88$ and (b) $\xi(n) = 0.85$ respectively.

2.5.6 Convergence performance of SC-IPNLMS for NEC

We provide additional simulations to illustrate the performance of SC-IPNLMS in the context of NEC. Figure 2.17 shows two network impulse responses, sampled at 8 kHz. The sparseness of these network impulse responses computed using (2.12) are (a) $\xi(n) = 0.88$ and (b) $\xi(n) = 0.85$ respectively. As before, we used a WGN input signal while another WGN sequence is added to give an SNR of 20 dB. Figure 2.18 shows the performances of NLMS, IPNLMS, for $\alpha_{\mathrm{IP}} = -0.5$ and -0.75, and the proposed SC-IPNLMS algorithm with $\alpha_{\mathrm{SC-IP}} = -0.75$. An echo path change was introduced using impulse responses as shown from Fig. 2.17 (a) to (b) at 2 s. We can see from the result that the performance of IPNLMS is dependent on α_{IP}. More importantly, a faster rate of convergence can be seen for SC-IPNLMS compared to NLMS and IPNLMS both at initial convergence and also after the echo path change.

2.6 Tracking performance under time-varying unknown echo system

As mentioned before, acoustic channels are inherently time-varying systems. It is therefore necessary to consider the performances of the adaptive algorithms under a time-varying system model.

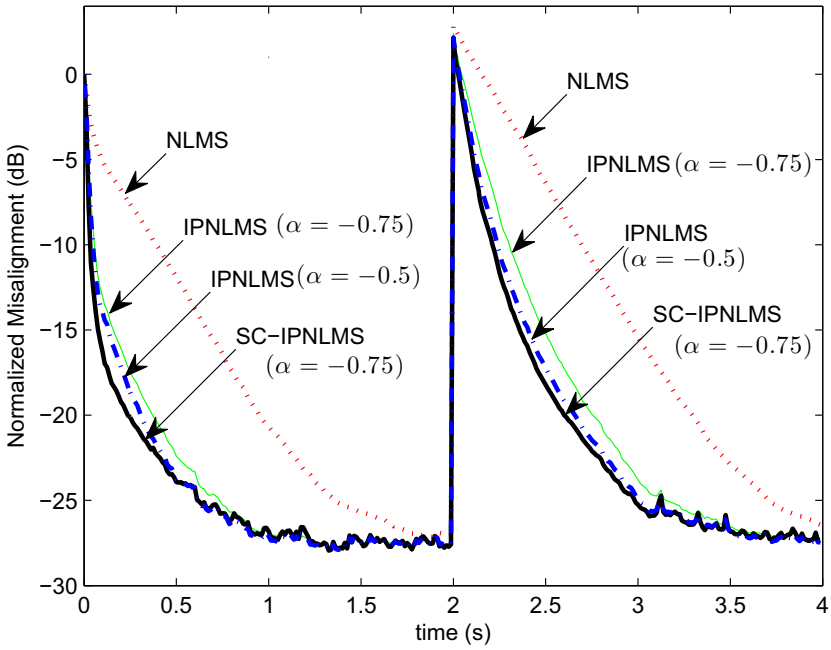

Figure 2.18: Relative convergence of NLMS, IPNLMS for $\alpha = -0.5$ and -0.75 and SC-IPNLMS using WGN input signal with an echo path change at 2 s. Impulse response is changed from that shown in Fig. 2.17 (a) to (b) and $\mu_{\text{NLMS}} = \mu_{\text{IPNLMS}} = 0.3$, $\mu_{\text{SC-IPNLMS}} = 0.7$, SNR = 20 dB.

2.6.1 Non-stationary echo system

First-order Markov model

If the channel changes slowly in time, it can be adequately represented by first order Markov channel [29]. The modified first-order Markov model [29] [30] is employed to represent a time-varying unknown system

$$\mathbf{h}(n) = \beta \mathbf{h}(n-1) + \mathbf{s}(n)\sqrt{1-\beta^2}, \tag{2.16}$$

where $\mathbf{s}(n)$ is an uncorrelated noise with elements drawn from a normal (Gaussian) distribution with zero mean and variance σ_s^2. $0 << \beta < 1$ controls the relative contributions to the instantaneous values of the "system memory" and "innovations" [29]. It can be noted that the greater β is the stronger the correlation of the sequence $\{\mathbf{h}\}$, and $\beta = 1$ represents a stationary environment.

Figure 2.19 shows the sparseness measure of the generated impulse responses with $L = 1024$, using the modified Markov model in (2.16) with parameters set to $\sigma_s^2 = 1$

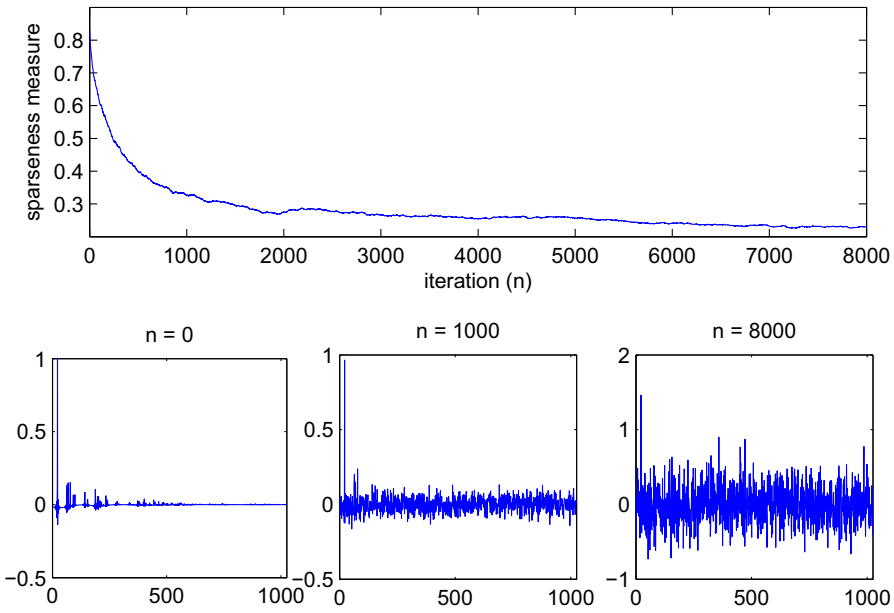

Figure 2.19: Sparseness measure of the generated impulse responses using the modified Markov model with $L = 1024$, $\sigma_s^2 = 1$ and $\beta = 0.9999$, against iteration number (n) and generated impulse responses at $n = 0, 1000$ and 8000, respectively.

and $\beta = 0.9999$, against iteration number (n). Even though these impulse responses cover approximately 70% of the sparseness range, the strength of the echo effects are not decaying at an exponential rate in magnitude for the later reflections, as can be noted from the impulses responses shown in Fig. 2.19.

Image model

A more realistic AIRs can be obtained using the method of image proposed in [25][26]. Figure 2.20 illustrates the sparseness measure of the generated impulse responses with $L = 1024$ against iteration number (n). For this illustration, we assumed that a loudspeaker is fixed at $4 \times 9.1 \times 1.6$ m inside a room with a dimension of $8 \times 10 \times 3$ m, and a user using a wireless microphone is moving away from the loudspeaker.

It can be noted that the bulk delay represented by the leading zeros in the impulse responses is proportional to the separation distance between the loudspeaker and the microphone at that particular time instance. Moreover, this cannot be modeled using the first order Markov model in Fig. 2.19 .

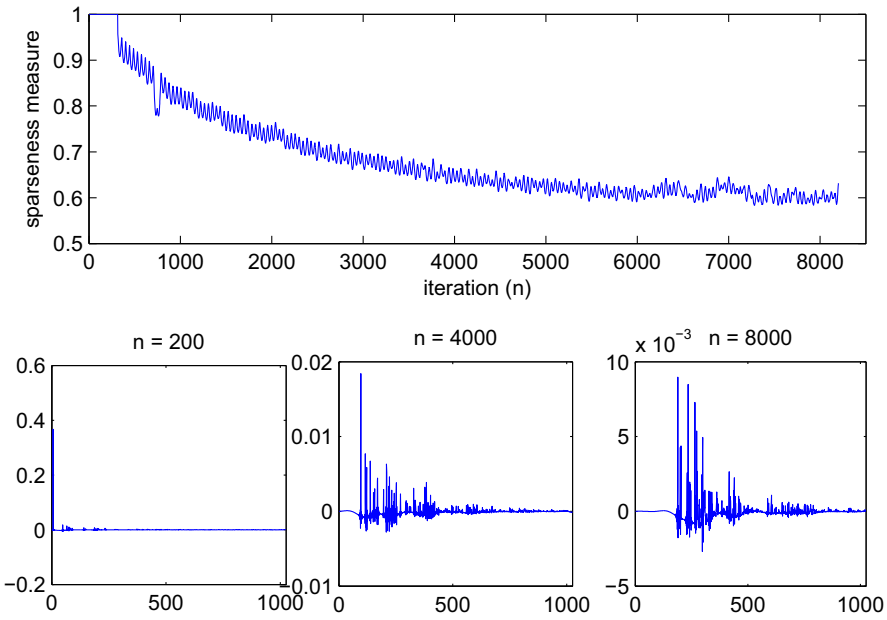

Figure 2.20: Sparseness measure of the generated impulse responses using the method of image with $L = 1024$ against iteration number (n) and generated impulse responses at $n = 200, 4000$ and 8000, respectively.

2.6.2 Simulation results

We present simulation results to compare the performances of the conventional and the proposed algorithms for time-varying system identification using the image model in the context of AEC. The input signal is zero mean WGN with $\sigma_x^2 = 1$ and the rest of the parameters were carried from the Section 2.5 simulations.

We chose to start these simulations with the impulse response generated at $n = 200$ in Fig. 2.20, which describes that the talker is 20 cm away from the loudspeaker. Inside NLMS, PNLMS, MPNLMS, IPNLMS, SC-PNLMS, SC-MPNLMS and SC-IPNLMS adaptations, every 40 iterations we switched to the next impulse response, which was generated when the wireless microphone has moved 1 mm further away from the fixed loudspeaker. Using 8 kHz as the sampling frequency, every 40 iterations is equivalent to every 5 ms, and therefore this setup is comparable to the microphone is moving at a constant velocity of 0.2 ms^{-1}.

Figure 2.21 - 2.23 illustrate the tracking performance of the algorithms under time-varying echo system. As it can be seen from the figures that the proposed algorithms gave

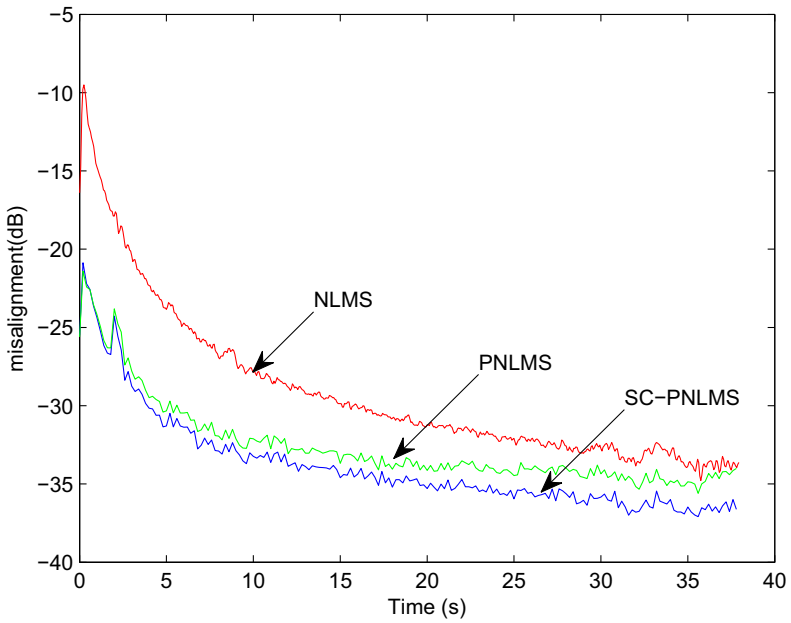

Figure 2.21: Relative tracking performances of NLMS, PNLMS and SC-PNLMS, using WGN input signal, under time-varying unknown system conditions simulated using the image model.

better tracking performances, compared to their conventional methods. These results reinforce our previous conclusions about the suitability of SC-PNLMS, SC-MPNLMS and SC-IPNLMS to build echo cancelers with improved robustness to echo system sparsity.

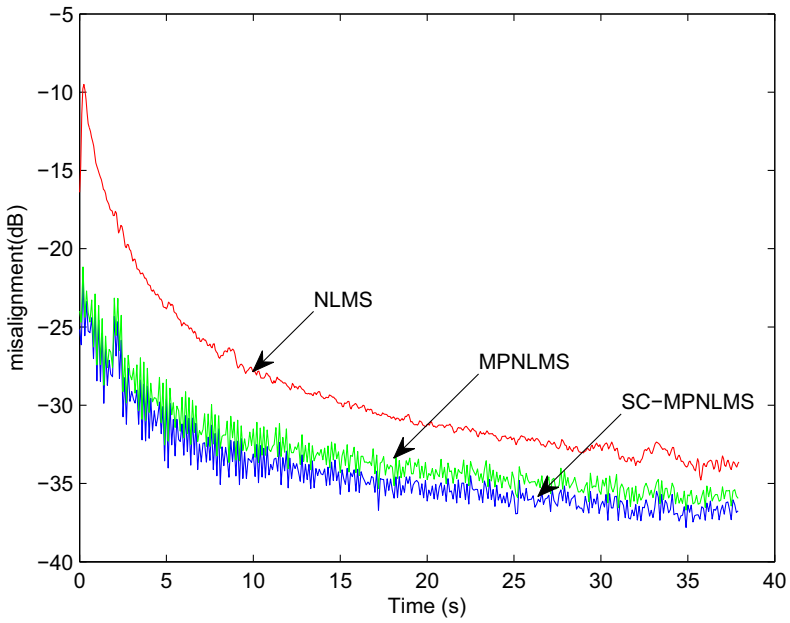

Figure 2.22: Relative tracking performances of NLMS, MPNLMS and SC-MPNLMS, using WGN input signal, under time-varying unknown system conditions simulated using the image model.

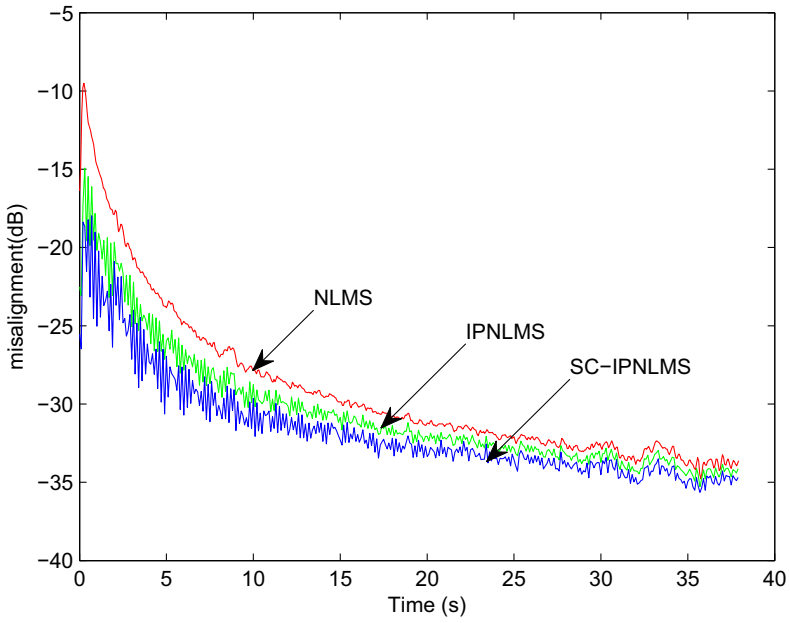

Figure 2.23: Relative tracking performances of NLMS, IPNLMS and SC-IPNLMS, using WGN input signal, under time-varying unknown system conditions simulated using the image model.

Chapter 3

Future Work

This chapter details the planning and time-line for implementation of the feasible future research areas. Some listed plans may be modified as we progress, in favor of more promising areas that may arise during the research.

3.1 Thesis Plan

Chapters in my final thesis will address the following topics:

- Chapter 1 - **Introduction**:

  A general introduction on the sparse algorithms and their uses in many different applications, along with their limitations within such applications, will be addressed in this chapter.

- Chapter 2 - **A class of sparseness controlled algorithms for echo cancellation:**

  This chapter will present the conventional sparse adaptive algorithms and the new class of AEC algorithms that can not only work well in both sparse and dispersive circumstances, but also adapt dynamically to the level of sparseness using a new sparseness-controlled approach drawing on techniques originally developed for NEC. It will also include the computational complexities of those algorithms, along with simulation results,

using WGN and speech input signals in order to compare performances over existing methods.

- Chapter 3 - **Mathematical analysis of sparse algorithms**

  The convergence performance of adaptive algorithms under time-invariant and time-varying unknown system conditions will be analyzed theoretically. So that, their performances at any particular instance in the convergence process can be predicted using the model. This is something that has some practical usefulness for setting the step-sizes and other parameters.

- Chapter 4 - **Sparseness-controlled in frequency / time-frequency domain**

  It is well-known that a sparse echo path can be identified faster than a dispersive echo path with same length. Therefore, transforming a dispersive echo path to a sparse path, using existing or possibly a new transformation, will improve the convergence speed of a dispersive system identification. This study will be included in this chapter.

- Chapter 5 - **Blind multi-channel identification**

  This chapter will include the detailed literature on the classical blind multi-channel identification. In a system with two microphones and one loudspeaker, it is interesting to study the relation between the two microphones. This chapter will include this study and possibly an extension of this work to M channels.

- Chapter 6 - **Conclusion**

  This chapter will conclude the remarks of the research and propose some possible extensions.

3.2 Research schedule

A detailed schedule relating to the proposed future works is shown in a Gaunt-chart as illustrated in Fig. 3.1.

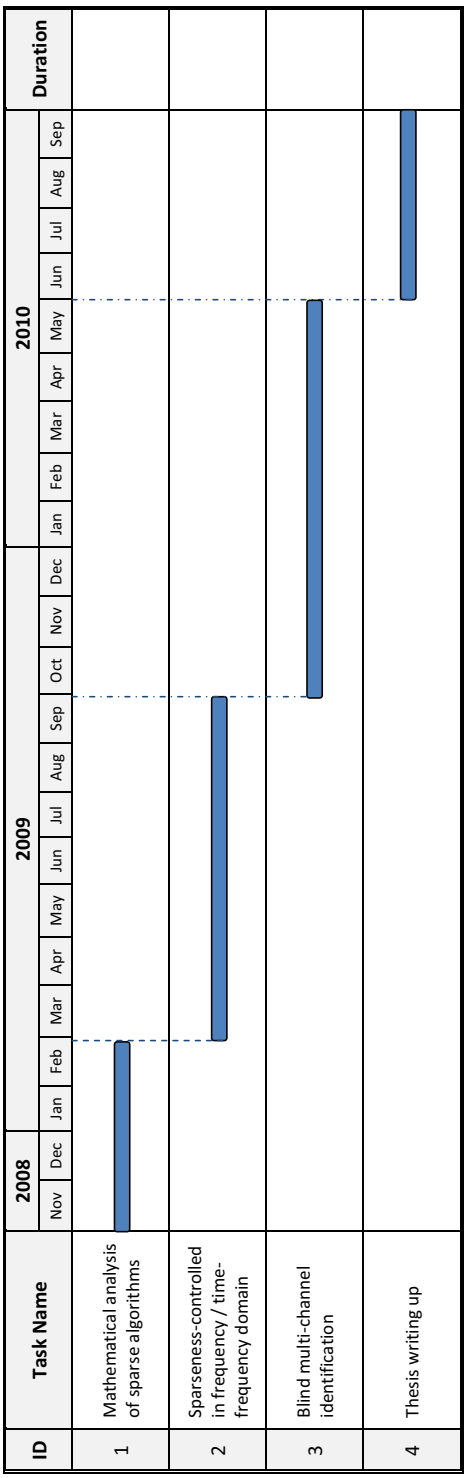

Figure 3.1: Research schedule.

Chapter 4

Conclusions

This report has addressed the significant problem caused by undesirable echoes that result from coupling between the loud speakers and microphones in the near end room. The research for this report has focused on the development of the adaptive filtering algorithms for sparse and dispersive systems, emphasising on the achievement of fast convergence rate with a modest increase in the computational cost.

We have presented a class of sparseness-controlled algorithms which achieves improved convergence compared to classical NLMS and typical sparse adaptive filtering algorithms. We have incorporated the sparseness measure into PNLMS, MPNLMS and IPNLMS for AEC to achieve fast convergence that is robust to the level of sparseness encountered in the impulse response of the echo path. The resulting SC-PNLMS, SC-MPNLMS and SC-IPNLMS algorithms take into account the sparseness measure via a modified coefficient update function.

It has been shown that the proposed sparseness-controlled algorithms are robust to variations in the level of sparseness in AIR with only a modest increase in computational complexity. Moreover, we have shown that these proposed algorithms have same or faster convergence in NEC and with time-varying echo system.

Finally, some feasible future work has been proposed according to the current demands in such fields.

Bibliography

[1] J. Radecki, Z. Zilic, and K. Radecka, "Echo cancellation in IP networks," in *Proc. Fourty-Fifth Midwest Symposium on Circuits and Systems*, 2002, vol. 2, pp. 219–222.

[2] S. Haykin, *Adaptive Filter Theory*, Information and System Science. Prentice Hall, 4th edition, 2002.

[3] A. W. H. Khong, J. Benesty, and P. A. Naylor, "Stereophonic acoustic echo cancellation: Analysis of the misalignment in the frequency domain," *IEEE Signal Processing Lett.*, vol. 13, no. 1, pp. 33–36, Jan. 2006.

[4] M. Doroslovacki and H. Fan, "Wavelet-based linear system modeling and adaptive filtering," *IEEE Transactions on Signal Processing*, vol. 44, no. 5, pp. 1156–1167, May 1996.

[5] R. H. Kwong and E.W. Johston, "A variable step-size algorithm for adaptive filtering," *IEEE Trans. Signal processing*, vol. 40, pp. 1633–1642, July 1992.

[6] C. Rusu and F. N. Cowan, "The convex variable step size (CVSS) algorithm," *IEEE Signal processing Letter*, vol. 7, pp. 256–258, Sep 2000.

[7] Junibakti Sanubari, "A new variable step size method for the LMS adaptive filter," in *IEEE Asia-Pacific Conference on Circuits and systems*, 2004.

[8] Bemard A. Schnaufer and W. Kenneth Jenkins, "New data-reusing lms algorithms for improved convergence," in *in Proc. Twenty-Seventh Asilomar Conf. Signals, Syst., Comput.*, 1993.

[9] Kyle A. Gallivan Robert A. Soni and W. Kenneth Jenkins, "Low-complexity data reusing methods in adaptive filtering," *IEEE Transactions on signal processing*, vol. 52, no. 2, pp. 394–405, Feb 2004.

[10] A. W. H. Khong and P. A. Naylor, "Selective-tap adaptive algorithms in the solution of the non-uniqueness problem for stereophonic acoustic echo cancellation," *IEEE Signal Processing Lett.*, vol. 12, no. 4, pp. 269–272, Apr. 2005.

[11] P. A. Naylor and A. W. H. Khong, "Affine projection and recursive least squares adaptive filters employing partial updates," in *Proc. Thirty-Eighth Asilomar Conference on Signals, Systems and Computers*, Nov. 2004, vol. 1, pp. 950–954.

[12] K. A. Lee and S. Gan, "Improving convergence of the NLMS algorithm using constrained subbands updates," *IEEE Signal Processing Lett.*, vol. 11, no. 9, pp. 736–739, Sept. 2004.

[13] R. Gray, "On the asymptotic eigenvalue distribution of toeplitz matrices," *IEEE Trans. Inform. Theory*, vol. 18, no. 6, pp. 725–730, Nov. 1972.

[14] D. L. Duttweiler, "Proportionate normalized least mean square adaptation in echo cancellers," *IEEE Trans. Speech Audio Processing*, vol. 8, no. 5, pp. 508–518, Sep. 2000.

[15] S. L. Gay, "An efficent, fast converging adaptive filter for network echo cancellation," November 1998, vol. 1, pp. 394–398.

[16] A. Deshpande and S. L. Grant, "A new multi-algorithm approach to sparse system adaptation," in *Proc. European Signal Process. Conf.*, 2005.

[17] J. Benesty and S. L. Gay, "An improved PNLMS algorithm," in *Proc. IEEE Int. Conf. Acoustics Speech Signal Processing*, 2002, vol. 2, pp. 1881–1884.

[18] A. W. H. Khong and P. A. Naylor, "Efficient use of sparse adaptive filters," in *Signals, Systems and Computers, 2006. ACSSC '06. Fortieth Asilomar Conference*, Oct 2006.

[19] Mojtaba Atarodi Mehran Nekuii, "A fast converging algorithm for network echo cancelation," *IEEE Signal Processing Letter*, vol. 11, no. 4, pp. 427–430, April 2004.

[20] Hongyang Deng and Milos Doroslovacki, "Improving convergence of the PNLMS algorithm for sparse impulse response identification," *IEEE Signal Processing Lett.*, vol. 12, no. 3, pp. 181–184, Mar. 2005.

[21] V. Gmez-Verdejo J. Arenas-Garca and A. R. Figueiras-Vidal, "New algorithms for improved adaptive convex combination of LMS transversal filters," *IEEE. Trans. Instr. Meas.*, vol. 54, pp. 22392249, 2005.

[22] Rehan Ahmad, Andy W.H. Khong, and Patrick A. Naylor, "Proportionate frequency domain adaptive algorithms for blind channel identification," in *Proc. IEEE Int. Conf. Acoustics Speech Signal Processing*, May 2006, vol. 5, pp. V29–V32.

[23] Gary W. Elko, Eric Diethorn, and Tomas Gänsler, "Room impulse response variation due to thermal fluctuation and its impact on acoustic echo cancellation," in *Proc. Int. Workshop on Acoustic Echo and Noise Control*, 2003, pp. 67–70.

[24] H. Sabine, "Room acoustics," *Transactions of the IRE Professional Group on Room Acoustics*, vol. 1, no. 4, pp. 4–12, Jul. 1953.

[25] J. B. Allen and D. A. Berkley, "Image method for efficiently simulating small-room acoustics," *J. Acoust. Soc. Amer.*, vol. 65, no. 4, pp. 943–950, Apr. 1979.

[26] P. M. Peterson, "Simulating the response of multiple microphones to a single acoustic source in a reverberant room.," vol. 80, no. 5, pp. 1527–1529, Nov 1986.

[27] Jacob Benesty, Yiteng (Arden) Huang, Jingdong Chen, and Patrick A. Naylor, "Adaptive algorithms for the identification of sparse impulse responses," in *Selected methods for acoustic echo and noise control*, Eberhard Hänsler and Gerhard Schmidt, Eds., chapter 5, pp. 125–153. Springer, 2006.

[28] Hongyang Deng and Milos Doroslovacki, "Proportionate adaptive algorithms for network echo cancellation," *IEEE Transactions on Signal Processing*, vol. 54, no. 5, pp. 1794–1803, May 2006.

[29] N. J. Bershad, S. McLaughlin, and C. F. N. Cowan, "Performance comparison of RLS and LMS algorithms for tracking a first order Markov communications channel," in *Proc. IEEE Int. Symposium on Circuits and Systems*, 1990, vol. 1, pp. 266–270.

[30] A. W. H. Khong and P. A. Naylor, "A family of selective-tap algorithms for stereo acoustic echo cancellation," in *Proc. IEEE Int. Conf. Acoustics Speech Signal Processing*, Mar. 2005, vol. 3, pp. 133–136.